Review Article

Nanostructured materials for solid-state hydrogen storage: A review of the achievement of COST Action MP1103

Elsa Callini [a,t], Kondo-Francois Aguey-Zinsou [b], Rajeev Ahuja [c,d],
Josè Ramon Ares [e], Sara Bals [f], Nikola Biliškov [g], Sudip Chakraborty [c],
Georgia Charalambopoulou [h], Anna-Lisa Chaudhary [i], Fermin Cuevas [j],
Bernard Dam [k], Petra de Jongh [l], Martin Dornheim [i], Yaroslav Filinchuk [m],
Jasmina Grbović Novaković [n], Michael Hirscher [o], Torben R. Jensen [p],
Peter Bjerre Jensen [q], Nikola Novaković [n], Qiwen Lai [b], Fabrice Leardini [e],
Daniele Mirabile Gattia [r], Luca Pasquini [s], Theodore Steriotis [h],
Stuart Turner [f], Tejs Vegge [q], Andreas Züttel [a,t], Amelia Montone [r,*]

[a] EPFL Valais Wallis - Swiss Federal Institute of Technology, LMER - Laboratory of Materials for Renewable Energy, Rue de l'Industrie 17, CH-1950 Sion, Switzerland
[b] MERLin Group, School of Chemical Engineering, The University of New South Wales, Sydney, NSW 2052, Australia
[c] Condensed Matter Theory Group, Department of Physics and Astronomy, Uppsala University, Box 516, Uppsala 75120, Sweden
[d] Applied Materials Physics, Department of Materials and Engineering, Royal Institute of Technology (KTH), S-100 44 Stockholm, Sweden
[e] Grupo Mire, Dpto. Fisica de Materiales, Facultad de Ciencias, Universidad Autonoma de Madrid, Spain
[f] EMAT, Department of Physics, University of Antwerp, Groenenborgerlaan 171, 2020 Antwerp, Belgium
[g] Ruđer Bošković Institute, Bijenička Cesta 54, 10000 Zagreb, Croatia
[h] National Center for Scientific Research "Demokritos", 15341 Ag. ParaskeviAttikis, Athens, Greece
[i] Department of Nanotechnology, Institute of Materials Research, Helmholtz-Zentrum Geesthacht, Max-Planck Strasse 1, Geesthacht, Germany
[j] ICMPE, UMR7182, CNRS-UPEC. 2-8 Rue Henri Dunant, Thiais 94320, France
[k] Chemical Engineering, Delft University of Technology, Julianalaan 136, 2628 BL Delft, The Netherlands
[l] Inorganic Chemistry and Catalysis, Debye Institute for Nanomaterials Science, Utrecht University, Universiteitsweg 99, 3584 CG Utrecht, The Netherlands
[m] Institute of Condensed Matter and Nanosciences, Université Catholique de Louvain, B-1348 Louvain La Neuve, Belgium
[n] Vinča Institute of Nuclear Sciences, University of Belgrade, POB 522, 1 000 Belgrade, Serbia
[o] Max Planck Institute for Intelligent Systems Stuttgart, Heisenbergstr. 3, 70569 Stuttgart, Germany
[p] Center for Materials Crystallography, Department of Chemistry and iNANO, Aarhus University, Langelandsgade 140, Aarhus C 8000, Denmark
[q] Department of Energy Conversion and Storage, Technical University of Denmark, Fysikvej, Building 309, DK-2800 Kgs. Lyngby, Denmark

[r] *Department of Physical Methods and Materials, ENEA, Research Centre of Casaccia, Via Anguillarese 301, Rome, Italy*

[s] *Department of Physics and Astronomy, Alma Mater Studiorum Università di Bologna, 40127 Bologna, Italy*

[t] *Empa, Swiss Federal Laboratory for Materials Science and Technology, Ueberlandstrasse 129, 8600 Duebendorf, Switzerland*

ARTICLE INFO

ABSTRACT

In the framework of the European Cooperation in Science and Technology (COST) Action MP1103 *Nanostructured Materials for Solid-State Hydrogen Storage* were synthesized, characterized and modeled. This Action dealt with the state of the art of energy storage and set up a competitive and coordinated network capable to define new and unexplored ways for Solid State Hydrogen Storage by innovative and interdisciplinary research within the European Research Area. An important number of new compounds have been synthesized: metal hydrides, complex hydrides, metal halide ammines and amidoboranes. Tuning the structure from bulk to thin film, nanoparticles and nanoconfined composites improved the hydrogen sorption properties and opened the perspective to new technological applications. Direct imaging of the hydrogenation reactions and *in situ* measurements under *operando* conditions have been carried out in these studies. Computational screening methods allowed the prediction of suitable compounds for hydrogen storage and the modeling of the hydrogen sorption reactions on mono-, bi-, and three-dimensional systems. This manuscript presents a review of the main achievements of this Action.

Contents

Introduction

Addressing climate change is an urgent worldwide problem and finding energy storage solutions for intermittent renewable energy sources is an essential alternative to current fossil fuel driven technologies. Current research focuses on the development of materials such as novel hydrogen storage (H-storage) materials to use hydrogen as an energy carrier. Hydrogen technology, such as production, storage and fuel cells, is a promising method of providing continuous non-polluting energy for a range of applications. Storing hydrogen as a solid in a metal matrix improves safety and efficiency when compared to compressed gas or liquid H-storage. However, several promising hydride materials have not yet found their way to the market, because they do not satisfy application-specific requirements, such as operating temperature/pressure, weight, reversibility and fast kinetics. Therefore, the mechanisms of hydrogen uptake and release to and from this matrix are of interest both from a fundamental scientific point of view and towards the development of hydrogen storage materials for practical use.

The ideal solid-state matrix for efficient hydrogen storage is the one, which can uptake and consequently desorb hydrogen at near ambient conditions. The prime focus of enhancing H-storage [1] capacity for such materials is to meet the gravimetric and volumetric density target set by Department of Energy (DOE) as 5.5 wt% hydrogen and 0.040 kg hydrogen/L [2]. From a gravimetric perspective, the storage material should be light to fulfill the DOE gravimetric density target. On the other hand, the lighter materials are facing problems of hydrogen desorption kinetics and/or reversibility. There is a combination of the covalent, ionic or van der Waals interactions involving strong or weak binding of hydrogen, respectively. The challenge of achieving the balance between the reaction enthalpies and the activation barriers for de- and re-hydrogenations reactions is the essential motivation behind hydrogen storage research in complex hydrides. For the chemisorption phenomena, the bottleneck is the strongly negative enthalpy of hydride formation, which can be increased usually at expense of the loss in volumetric and gravimetric capacities.

The impact and the importance of this topic required the creation of specific tasks to address both fundamental and technological questions. The COST Action MP1103 *Nanostructured Materials for Solid-State Hydrogen Storage* (SSHS) represents the largest consortium of scientists working in the framework of the European Union on hydrogen storage. In the past 4 years, the Action moved towards the use of SSHS in current technologic applications.

This paper represents a review and an overview of the main achievements of the Action in terms of synthesis of novel materials, innovative characterization methods and theoretical tools to model the H-sorption reaction and design new improved materials.

The rest of this manuscript is divided into three sections representing the main tasks of the COST Action MP1103, shortly introduced in the following.

Synthesis of novel materials and systems for SSHS

The synthesis of innovative materials with specific H-sorption properties is the first step towards the development of efficient H-storage systems. These materials are required to have *i)* high gravimetric and volumetric H-storage capacities, *ii)* suitable thermodynamics at operation conditions, *iii)* fast H-uptake and release, *iv)* long-term cycling stability, *v)* low cost, and *vi)* environmental friendliness. For attaining high gravimetric performance, the use of light-elements is mandatory [3,4]. As a consequence, recent research activities mainly focused on the synthesis of magnesium-based materials, complex hydrides (alanates, borohydrides and imides-amides), carbon and metal-organic-frameworks porous materials, as well as composite and hybrid materials made up of the former material classes. Unfortunately, the mobility of hydrogen in these compounds is usually slow as result of the ionic and covalent bonds formed by hydrogen atoms. To speed-up the reversible H-sorption processes, material nanostructuration should be pursued to shorten diffusion paths and increase the density of chemisorption sites. In some particular cases, material downsizing to the nanoscale may also modify the hydrogen thermodynamics for tuning to operation conditions.

Characterization methods for novel materials and systems for SSHS

Analysis and characterization of new materials and storage systems, including metal organic framework (MOF) materials, metal hydride powders and thin films, and the tanks in which these materials are stored, pose new challenges due to the sensitive nature of the materials themselves. These challenges include accurate measurement of H-storage capacities, determination of phase evolution during H-sorption, thermal, structural and morphological analysis, and characterization of materials and heat transfer processes inside a storage tank. This section outlines characterization methods that address some of the challenges involved with novel H-storage materials.

Computational methods for novel materials and systems for SSHS

Computational modeling is largely used to study, search for, and predict new materials for SSHS. The computational

methods have improved greatly over the last decades, now providing predictive accuracy in terms of thermodynamic and structural properties, as well as identification of reaction pathways and temperatures at a computational speed suitable for investigating multiple compositions and/or complex structures covering a range of different physical phenomena and processes [5—10]. Using computational methods, e.g. at the density functional theory (DFT) level [11,12], it is possible to obtain knowledge about the atomistic details of materials, which might not be available using standard experimental procedures, but important to describe and optimize a reaction or transport mechanism [13]. Furthermore, it is possible to perform large-scale screening studies of e.g. the stabilization/destabilization effects that different alloys, mixtures and dopants would have on a SSHS material, without the need of synthesizing all possible combinations [14]. This approach reduces the number of experimental screening tests, facilitating environmentally friendly and cost-saving computational materials design and optimization.

Synthesis of novel materials and systems for H_2 storage

Different material nanoarchitectures deserve interest either for mechanistic understanding or for H-storage applications. This applies to powders, thin films, nanorods and nanoparticles which are prone to absorb hydrogen in atomic or ionic form. On the other side, nanoporous materials can adsorb hydrogen molecules by van der Waals forces on their large internal surface area. Additionally, these porous materials can be used as scaffolds to confine nanoparticles and avoid their coalescence. Specific synthetic routes for the design of such kinds of material architectures are surveyed in the following.

Nanostructured bulk materials

Three-dimensional nanostructured materials can be obtained by the use of severe plastic deformation techniques. In particular, mechanochemical synthesis has become one of the most utilized methods for the preparation of nanostructured hydride materials. Moreover, the direct synthesis of nanohydrides from the elements can be achieved by milling under hydrogen atmosphere [15]. Hydride formation can be monitored in situ using special vials equipped with pressure and temperature sensors [16]. This direct synthetic route has been successfully applied to the synthesis of binary hydrides (MgH_2, TiH_2) [15,17], magnesium complex hydrides (Mg_2FeH_6, Mg_2CoH_5, Mg_2NiH_4, $Mg_2(FeH_6)_{0.5}(CoH_5)_{0.5}$) [16,18—21], alkali alanates ($NaAlH_4$, Na_3AlH_6, Na_2LiAlH_6, K_2LiAlH_6, $KAlH_4$) [22—26] and lithium amide [27]. Compound formation is typically achieved in less than 3 h with reaction yields above 90%. Up to 10 g of material can be prepared in a single experiment and higher amounts can be industrially envisaged by implementation of continuous flow processes. This technique also allows one-pot synthesis of catalyzed nanohydrides such as Ti-doped alanates [28] and MgH_2–TiH_2 nanocomposites [29]. To illustrate the architecture obtained for the latter system, Fig. 1 displays the microstructure of $0.7MgH_2$-$0.3TiH_2$

nanocomposites prepared by mechanochemistry of Mg and Ti powder mixtures at $p(H_2) = 80$ bar. The nanocomposites consist of micrometric-size MgH_2–TiH_2 agglomerates in which 10 nm in size TiH_2 inclusions are homogeneously distributed in MgH_2 matrix. These inclusions limit Mg grain growth during reversible hydrogen cycling and favor H-mobility within the composite [30]. Loose powders obtained by mechanochemistry should be compacted for the implementation of hydrogen storage tanks [31].

Mechanochemistry under selected gas can be applied to the synthesis of a wide range of hydrides thermodynamically stable at the selected synthesis conditions, i.e. hydrogen pressures up to 150 bar, macroscopic temperatures below 100 °C but may locally be significantly higher [32]. Heat development and increasing temperatures may be reduced by pauses during mechanochemical treatment [33]. Moreover, mechanochemical synthesis of borohydrides may be safely conducted in diborane B_2H_6 gas, which provided a new route to halide and solvent free metal borohydrides [34—36]. Mechanochemical synthesis has provided a range of novel bi- and tri-metallic borohydrides, which may not be prepared by other means, e.g. based on rare earths metal, new families of perovskite type compounds or fast lithium ion conductors [37—45]. In other cases, metal borohydrides may form eutectic low melting mixtures, e.g. $0.725LiBH_4$–$0.275KBH_4$ with melting point at $T = 105$ °C [46—48].

Some of the hydrides cannot be prepared by standard ball milling procedures either due to the highly exothermic self-accelerating reactions, as those occurring in the preparation of lithium and sodium hydrazinidoboranes [49,50], or due to the safety concerns as for example related to the use of aluminum borohydride, or due to the low stability of the reacting components. In such cases, careful manual grinding, or repetitive soaking/grinding as for the case of $K[Al(BH_4)_4]$ [51], or cryo-ball milling as for the case of $NH_4Ca(BH_4)_3$ [43,52] are used.

Solvent based methods are very useful to prepare new halide-free mono-metallic borohydrides for precursors for pure bi- or tri-metallic borohydrides [53,54]. A range of metal borohydride solvates has also been discovered, e.g. [{Li(Et$_2$O)$_2$}Mn$_2$(BH$_4$)$_5$] and [{Na(Et$_2$O)$_2$}Mn$_2$(BH$_4$)$_5$] crystallize in the monoclinic space groups $C2/c$ and $C2$, respectively as intermediates during synthesis of $Mn(BH_4)_2$ [55]. The monoclinic solvates $M(BH_4)_3 \cdot S(CH_3)_2$ (M = Y or Gd) transform to α-$Y(BH_4)_3$ or $Gd(BH_4)_3$ at about 140 °C as verified by thermal analysis [47]. Reductive synthesis in ether followed by solvent extraction is also useful, e.g. for synthesis of $Eu(BH_4)_2$ and $Sm(BH_4)_2$ [53]. A new method for synthesis of ammine metal borohydrides, which combine mechanochemistry, solvent based methods and solid—gas reactions has provided a wide range of materials with varying compositions, e.g. $M(BH_4)_3 \cdot nNH_3$, M = Y, Gd, Dy; $n = 7, 6, 5, 4, 2$ and 1 [56,57]. Metal borohydrides may also be combined with other neutral molecules such as amidoborane and mechanochemical treatment of α-$Mg(BH_4)_2$ and NH_3BH_3 provides $Mg(BH_4)_2 \cdot 2NH_3BH_3$ [58]. Direct interaction of the volatile aluminum borohydride and NH_3BH_3 yields $Al(BH_4)_3 \cdot NH_3BH_3$, where the Al-coordinated ammonia borane releases two H_2 molecules per Al already at 70 °C [59]. Contrary to that of the pristine ammonia borane and to its other complexes with metal borohydrides, this process is endothermic,
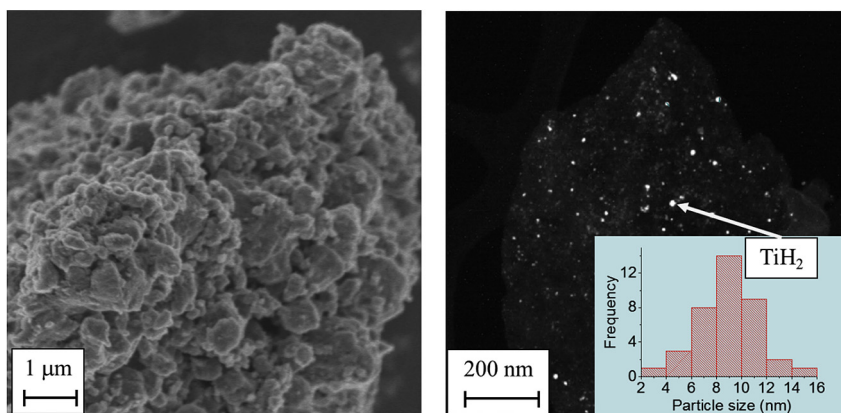
Fig. 1 – Microstructure of $0.7MgH_2$–$0.3TiH_2$ nanocomposites. Left: SEM micrograph. Right: TEM image in dark field mode showing the homogeneous dispersion of TiH_2 inclusions in MgH_2 matrix.

suggesting a possibility for direct rehydrogenation. Other Al-based Lewis acids, less challenging with respect to the stability and safety than $Al(BH_4)_3$, may be good agents for supporting the reversible dehydrogenation of NH_3BH_3 under mild conditions.

Another way of preparing hydrides with high volumetric hydrogen density is the use of a high hydrostatic pressure. Already at pressures of 1 GPa, achievable in laboratory steel dies, the amorphous $Mg(BH_4)_2$ can be synthesized [60], as well as the dense form of $Mn(BH_4)_2$ [61]. Both phases can be quenched to ambient pressure.

Nanostructured bulk materials can also be prepared by a physical bottom-up approach, where the gas-phase condensation technique is employed to grow nanoparticles from metal vapors, followed by in situ collection and cold-compaction of the nanoparticles. Using two or more vapor sources, alloys or nanocomposites can be obtained even starting from immiscible elements, as recently demonstrated for the Mg–Ti immiscible couple [62]. Mg–Ti nanostructures prepared this way exhibit extremely fast hydrogen sorption kinetics even at Ti contents lower than 10 wt%.

Thin films

Thin films provide a means to analyze the effect of surface energy, strain and plastic deformation on the hydrogenation kinetics and thermodynamics in a controlled way. Nano-sizing may result in a modification of all three terms, which makes it often difficult to estimate the contribution of these terms to destabilization aimed for. However, it should be stressed that the first two effects give a shift in both branches of the hysteresis, while plastic deformation results in widening of the hysteresis. Therefore, one cannot conclude much on the basis of a shift in the plateau pressure of only one of the branches.

Using a Ti/Mg/Ti/Pd multilayer thin film with a gradient Mg thickness Mooij et al. [63] found that the hydrogenation plateau pressure depends on the thickness. They deduced this to be the result of a change in the Mg/Ti interface energy on hydrogenation of around $0.35 J/m^2$. From similar experiments on Fe/Mg/Fe/Pd multilayers [64] a much higher interface energy was deduced, although the effect was partly obscured by the diffusion of Pd through Fe. Strain plays only a minor role on the plateau pressure of MgH_2 in this multilayer system.

Plastic deformation mainly affects the kinetics of the hydrogenation of Mg in the multilayer Ti/Mg/Ti/Pd system. Optical transmission images of the films taken at a pressure slightly below the hydrogenation plateau, clearly shows the nucleation and growth behavior of Mg starting from preferential nucleation sites (Fig. 2). From an analysis of the relation between the step curvature and the expansion of the nucleating islands, the reduction of the kinetics due to the plastic deformation could be quantified [65,66]. We expect that such a reduction in the kinetics also takes place in melt-infiltrated nanocrystals, which are bound to be strongly affected by plastic deformation.

Porous materials

H-storage by physisorption of hydrogen molecules requires high specific surface areas [67]. For decades the best crystalline materials have been zeolites with about 900 $m^2 g^{-1}$ and the largest surface areas have been achieved by disordered activated carbons with around 3000 $m^2 g^{-1}$. The field of cryoadsorption gained new momentum due to the development of a novel class of crystalline lightweight materials with extremely high porosity, the so-called metal-organic frameworks (MOFs), which are almost exclusively synthesized by hydrothermal or solvothermal techniques. After removing the solvent, these frameworks are stable exhibiting a permanent nanoporosity and reaching specific surface areas of up to 5000 $m^2 g^{-1}$ [68]. The full characterization of these structures and their hydrogen uptake requires typically measurements at different temperatures and high pressures. Recently, a new measuring procedure operated at low pressure and near the boiling point of hydrogen was developed, which enables to determine the physical upper limit of hydrogen uptake and the BET apparent surface area with one low-pressure isotherm [69,70]. Owing to their low heat of adsorption, these materials have to be mainly operated around liquid
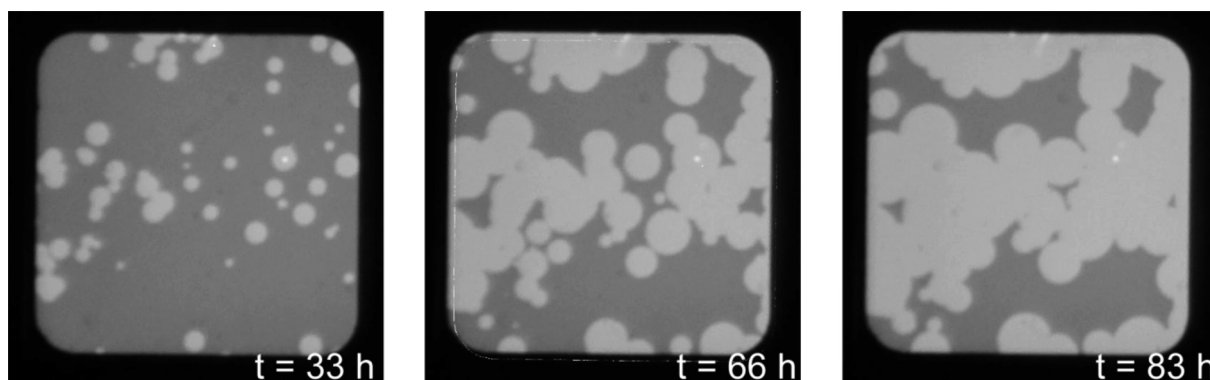
Fig. 2 – Images of the 10 × 10 mm thin film Ti/Mg/Ti/Pd multilayer samples in optical transmission after multiple hours of exposure to hydrogen (p_{H2} = 70 Pa, T = 363 K). The MgH$_2$ domains transmit more light and are brighter. Over time, the islands grow bigger, while new nuclei are still being formed.

nitrogen temperature to reach high storage capacities. Synthesis of frameworks containing unsaturated metal sites [71] or by linker modification [72] may help to improve the interaction with hydrogen and increase the heat of adsorption. Recently, modifications of hydrides with permanent porosity have been synthesized, which can additionally host smaller guest molecules such as H$_2$, N$_2$ or CH$_2$Cl$_2$, denoted γ−Mg(BH$_4$)$_2$ and γ−Mn(BH$_4$)$_2$ [54,73]. These novel structures are hybrids of hydrides and physisorption materials which in principle can reach extremely high, although non-reversible, hydrogen densities. Nanoporous materials can also act effectively to host metal hydride nanoparticles for reversible hydrogen storage, as discussed in more detail in the next paragraph.

Nanoparticles and nanoconfined hydrides

A strategy to improve the kinetic and thermodynamic properties of hydride materials is through particle size reduction. It is well known that the physicochemical properties of materials change when particles size reaches a few nanometers [74,75]. An archetypical example is gold, which becomes a very effective catalytic material once particle size reaches 10−20 nm [76].

Upon particles size reduction, hydride materials are expected to display faster H-sorption kinetics due to shorter diffusion paths, but also to the higher surface area exposed to hydrogen. More importantly, reduction in particle size may lead to a positive or negative alteration of the thermodynamic properties, i.e. a stabilization or destabilization of the hydride [77−80]. The driving forces for these changes are mainly understood in term of excess of surface energy. Hence, if the nanosized metal hydride particle has a higher surface energy than the corresponding non hydrided metal particle, hydrogen desorption will be facilitated at low temperatures.

However, establishing an effective method for the synthesis of small, well defined and stabilized light metal hydride nanoparticles has posed a great challenge. The possible approaches are illustrated in Fig. 3. Wet chemical synthesis in solution yields isolated nanoparticles, and examples developed from the earliest reports on Mg nanoparticles in the

1980's to now include also complex metal hydride nanoparticles and core−shell structures. Even more recently, methods based on porous hosts have started to emerge. Solution-based impregnation generally yields supported nanoparticles, while melt infiltration with complex metal hydrides rather yields composites in which the scaffold pores are completely filled with nanoconfined material. More recently more complicated hydride composites have been pore-confined or co-infiltrated. For practical applications, it is important to maximize the hydride loading of the scaffold.

Gas-phase condensation permits the synthesis of metal and alloy nanoparticles with a good control on their average size and a high purity [81−83]. Individual nanoparticles can be collected on suitable substrates for model studies of H-sorption by optical transmission, as discussed for thin films [84]. The formation of a continuous shell by, e.g. reaction with oxygen prevents coarsening phenomena and naturally yields core−shell metal-oxide systems [85]. Alternatively, co-evaporation of a second phase effectively suppresses nanoparticle coarsening [62].

Although a full understanding of the behavior of hydrogen in nanosized hydrides has not been reached to date, remarkable progress has been made in recent years and several marking features can be highlighted:

(i) Generally particle size reduction leads to a drastic improvement in kinetics, and hence a reduction of the hydrogen desorption temperature. For example, supported MgH$_2$ nanoparticles released hydrogen at 200 °C instead of the 400 °C for bulk magnesium, and most of the hydrogen content could be absorbed within 5 min at 300 °C compared to 60 min for ball-milled magnesium [86−88]. NaAlH$_4$ supported on carbon showed room temperature hydrogen desorption instead of the 250 °C for bulk NaAlH$_4$ [89,90]. Similarly, lower desorption temperatures have been found for LiBH$_4$ and NaBH$_4$ [91,92].

(ii) Particle size reduction also enables reversibility. Hence, many complex hydrides non-reversible under practical conditions, show some degree of, or even full,
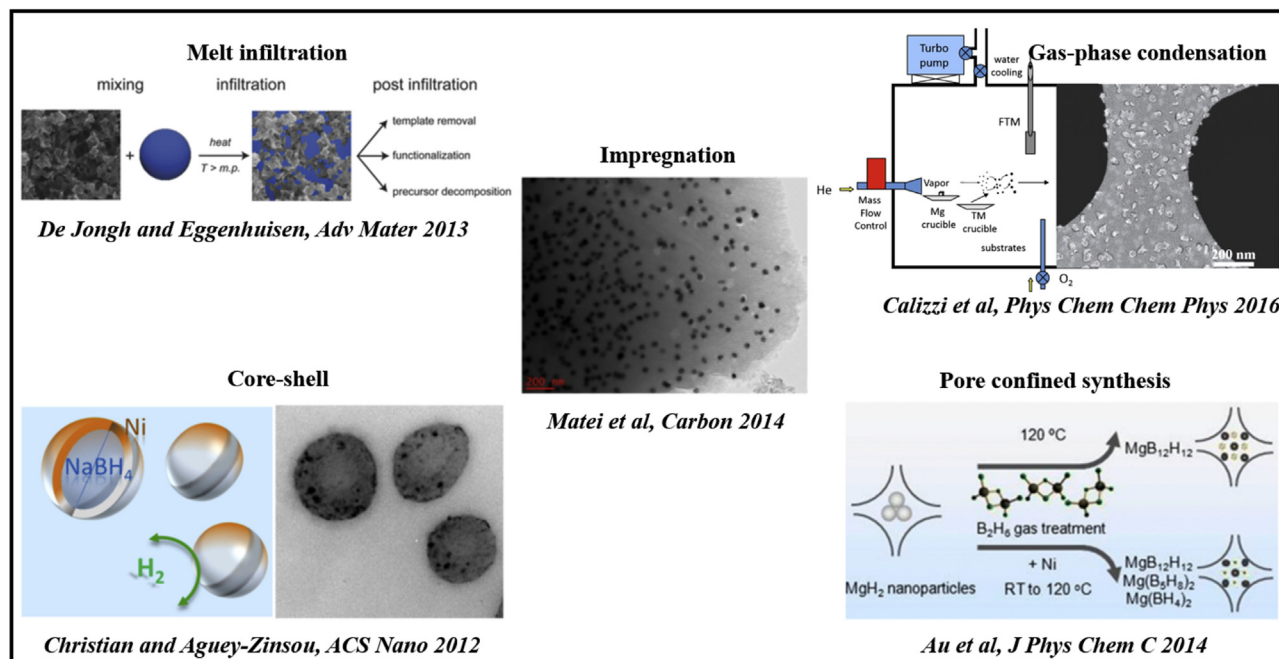
Fig. 3 – Selected examples of synthetic approaches for confined hydrides [74,75,77–80].

reversibility under relatively mild conditions and without a catalyst upon particle size reduction and/or confinement. This is particularly the case for $NaBH_4$ [93,94], $LiBH_4$ [92], and $NaAlH_4$ [95,96].

(iii) Particle size reduction, and interaction with the scaffold pore walls, is likely to modify thermodynamic paths. For example, confined ammonia borane shows little by-products in the form of borazine or ammonia [97]. While for ionic hydrides such as MgH_2 the hydride will become relatively less stable upon particle size reduction, for complex metal hydrides such as $NaAlH_4$, which have lower surface energies than their decomposition products, instead the nanosized hydrides may become more stable [98].

(iv) In core–shell systems, the shell may mechanically constrain the volume changes, which the core undergoes upon hydrogen sorption. Simple calculations show that the resulting elastic strain can induce relevant thermodynamic changes, such as hydride destabilization [84]. The onset of plastic deformation, however, can strongly reduce this effect, giving rise to a large pressure hysteresis between absorption and desorption.

New amidoboranes

The exploration of new compounds is the starting point to select suitable candidates for SSHS. Recently, ammonia borane (NH_3BH_3) has been extensively investigated due to its extremely high gravimetric and volumetric hydrogen density. However, serious drawbacks make it an unfavorable system for practical onboard hydrogen storage. Its reactivity is largely determined by intermolecular dihydrogen bonding

interaction of N-H$^{\delta+}\cdots^{\delta-}$H-B type, which operates in solid NH_3BH_3. Thus, the flexibility of this interaction is of crucial importance for fine-tuning of properties of NH_3BH_3-based systems. A very successful approach is its chemical modification by substitution of one H$^{\delta+}$ of NH_3 moiety by an electropositive element, such as alkaline or alkaline earth metal, which gives rise to amidoboranes [99]. This substitution causes a significant destabilization of dihydrogen bonding network, with assistance of dehydrogenation via hydride transfer by intermediate MH species. The changes in dehydrogenation mechanism, as well as opportunity of tuning of thermodynamics [100] make them highly promising systems for hydrogen storage2. Additionally, complexation of amidoboranes with hydrogen bond donating species, such as NH_3 [101] or NH_3BH_3 [102] further promotes dehydrogenation.

Seen these facts, it is therefore extremely important to synthesize and characterize new NH_3BH_3-based materials. Specifically, in the framework of the COST Action MP1103, synthesis and characterization of a bimetallic NH_3BH_3-based compound was successfully achieved: $Li_2Mg(NH_2BH_3)_4$. As comparison, $Na_2Mg(NH_2BH_3)_4$ [103] was synthesized under the same conditions, starting from NH_3BH_3 and NaH.

Fig. 4 presents combined evidence from IR spectra and XRD for $Li_2Mg(NH_2BH_3)_4$: its structure was solved by Rietveld refinement [104] and it shows that the bonding in this system is very similar, but not isostructural to $Na_2Mg(NH_2BH_3)_4$. These structural measurements determine the coordination of cations, revealing similar behavior of Li^+ and Na^+: each Mg^{2+} is tetrahedrally bonded to N of four NH_2BH_3 groups, while each Li^+/Na^+ is octahedrally coordinated to the BH_3 units of six NH_2BH_3 groups [103].

Recently, numerous metal amidoboranes, including the mixed-metal compounds $Na[Li(NH_2BH_3)_2]$ [105] and $Na_2[Mg(NH_2BH_3)_4]$ [103], were obtained and characterized.
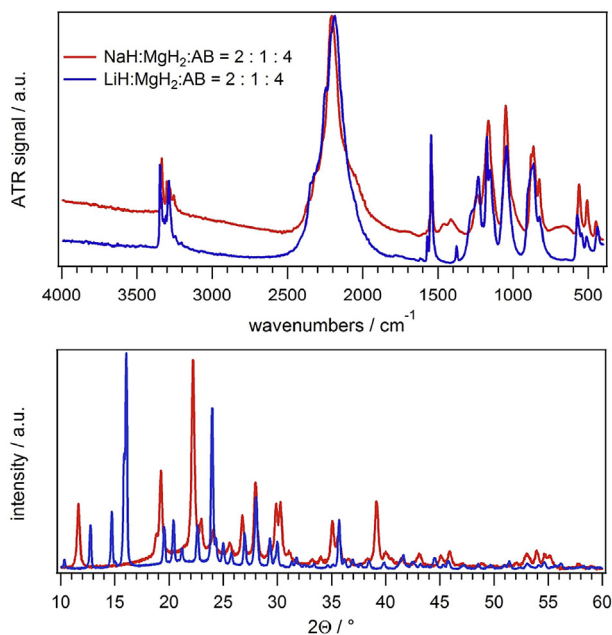
Fig. 4 – IR (top) and XRD (bottom) of $Li_2Mg(NH_2BH_3)_4$ (blue) and $Na_2Mg(NH_2BH_3)_4$ (red) as comparison. (For interpretation of the references to color in this figure legend, the reader is referred to the web version of this article.)

Although most of the metal amidoboranes release NH_3 and NH_2BH_2 in addition to hydrogen, $LiNH_2BH_3 \cdot NH_3BH_3$ produces up to 14.0 wt % of pure hydrogen upon heating to 230 °C [102]. The first Al-based amidoborane, $Na[Al(NH_2BH_3)_4]$, has been obtained mechanochemically and characterized in detail recently [106]. Reaction of the hydrides $NaAlH_4$ and NH_3BH_3, splitting hydrogen, was possible due to both the lower stability of the Al–H bonds compared to the B–H ones in borohydrides, and due to the strong Lewis acidity of Al^{3+}. On heating, $Na[Al(NH_2BH_3)_4]$ releases in two steps 9 wt % of pure hydrogen and the amorphous product can reversibly adsorb a part of the released hydrogen at 250 °C and $p(H_2) = 150$ bar. The composite $NaAlH_4–4NH_3BH_3$ might become a starting point towards a new series of aluminum-based tetraamidoboranes with improved hydrogen storage properties. This series can be extended in particular using synthesis in solutions, for example in THF.

These results open a new possibility for storing hydrogen in solids and confirm the importance of structural investigations for the validation of the synthesis procedures.

Characterization methods for novel materials and systems for H₂ storage

Metal-organic framework materials and direct imaging techniques

Metal-organic frameworks (MOFs) are a relatively new class of porous materials, consisting of metal ion centers linked together by organic linkers to create flexible but crystalline porous networks. In recent years, MOFs received huge attention because of their high specific surface areas and pore volumes, applicable in catalysis, photovoltaics and especially in gas (H_2) storage [107,108]. For specific applications MOF crystals can be loaded with catalytically active materials like Au, Pt and Ru in the form of nanoparticles, small clusters or single atoms, leading to an increased activity in e.g. olefin hydrogenolysis and methanol synthesis, or with semiconductor nanomaterials like GaN or ZnO for improved optical properties [107]. In H-storage applications, hydride-forming materials, like Pd, can also be loaded into the frameworks in the form of nanoparticles, in order to boost the storage capacities.

Structural characterization of this type of extremely delicate materials and their interaction with extra-framework guests remains extremely challenging. Most of the common characterization techniques such as X-ray diffraction or nitrogen adsorption for this type of materials only offer global structural information, and cannot provide direct information
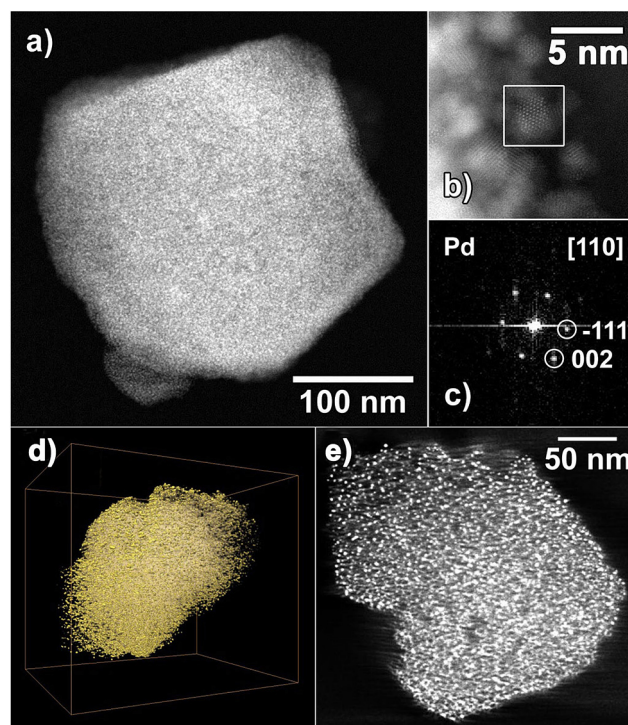
Fig. 5 – a) HAADF-STEM of Pd@COF-102; the image reveals the even distribution of Pd particles throughout the COF-102 framework; b) HRHAADF-STEM image of a Pd nanoparticle imaged along the [110] zone axis at atomic resolution; c) Fourier transform of the area highlighted by the white frame in b) showing evidencing that the particle in b) is cubic Pd(0); d) Tomographic reconstruction of Pd@COF-102. The Pd nanoparticles are rendered in gold, the COF framework in soft off-white; e) Orthoslice through the three dimensional reconstruction of a loaded Pd@COF-102. The particles visible as white dots are clearly present in the whole crystals without any preferential distribution in size or position.

on e.g. the distribution of embedded nanoparticles. Transmission electron microscopy is an ideally suited technique for this purpose, as it can provide structural information down to atomic resolution. Furthermore, technological advances including aberration-correctors, low-voltage techniques, cooling holders, beam-blanking systems and fast-readout cameras nowadays do allow pore imaging of most types of MOFs by TEM [109].

A recent example of the characterization of this type of material is presented in Fig. 5 [110]. In this work, covalent organic frameworks (3D), a metal-free subclass of the metal-organic frameworks, were demonstrated as a new class of novel templates for the deposition of hydride-forming Pd nanoparticles. Photo decomposition of a $[Pd(\eta^3\text{-}C_3H_5)(\eta^5\text{-}C_5H_5)]$@COF-102 inclusion compound (synthesized via gas phase infiltration method) led to the formation of a Pd@COF-102 hybrid material. Advanced electron microscopy techniques (including high-angle annular dark field images in scanning transmission electron microscope mode and electron tomography) along with other conventional characterization techniques unambiguously showed that highly monodispersed Pd nanoparticles (2.4 ± 0.5 nm) were evenly distributed inside COF-102 framework. The Pd@COF-102 hybrid material discussed in this work was one of the very rare examples of metal nanoparticles loaded porous crystalline materials with a very narrow size distribution without any larger agglomerates even at high loadings (30 wt%). Two samples with moderate Pd content (3.5 wt% and 9.5 wt%) were used to study the H-storage properties of the metal decorated COF surface. The uptake of hydrogen at room temperature from these samples was significantly higher than similar systems such as Pd@MOF. The study showed that the H_2 capacities were enhanced by a factor of 2–3 via Pd impregnation on COF-102 at room temperature and 20 bar. This remarkable enhancement was not only due to Pd hydride formation, but also to hydrogenation of residual organics such as bicyclopentadiene. The significantly higher reversible H-storage capacity that came from decomposed products of the employed organometallic Pd precursor suggested that our discovery may be relevant to the discussion of the spill-over phenomenon in metal@MOF and related systems.

It is interesting to note in this context that light complex hydrides are very sensitive to electron beams. However, complete structural information, including the location of the H atoms, can be obtained from submicrometer-sized crystallites, as illustrated on the example of $LiBH_4$ [111], using precession electron diffraction at low-dose conditions.

Gas sorption measurement techniques

Basic hydrogen storage properties of practical interest for solid materials, namely (a) sorption capacity, (b) kinetic properties, (c) enthalpy of sorption, (d) cycling stability, can be assessed using gas sorption based experimental techniques, either manometric or gravimetric [112]. In principle, manometric and gravimetric techniques provide the same information, however as they are based on different concepts, discrepancies are often observed. As such, the combination of volumetric and gravimetric measurements is often required for the reliable assessment of a material's H-storage properties.

Both types of methods allow the measurement of the up-taken/desorbed amount of gas at pre-selected temperatures (e.g. from 20 to 600 K), as a function of pressure (e.g. up to 150 bar), while monitoring simultaneously the kinetics of gas sorption at each pressure step.

The most technologically relevant property determined through such methods is the reversible H-storage capacity of a material, defined as the quantity of hydrogen up-taken and desorbed between the respective lower and upper operating pressures. In the case of hydrides the reversible storage capacity can be deduced by the width of the plateau in the so called Pressure–Composition Isotherm (PCI) curve, that are obtained by measuring the changes in hydrogen pressure and corresponding evolution of the hydrogen content in the hydrogen/metal system (expressed as hydrogen-to-host atomic ratio, H/X) at a given temperature. By performing a set of isotherms at different temperatures, it is possible to deduce the enthalpy change, ΔH, associated with the hydriding/dehydriding reaction, comprising a fundamental measure of the metal–H bond strength, especially important for the heat management required when considering practical applications. For almost all hydrides, the absorption plateau pressure increases with temperature, following in general the van 't Hoff relation:

$$\ln p/p^0 = \frac{\Delta H^0}{RT} - \frac{\Delta S^0}{R}$$

where p is the hydrogen pressure, ΔH^0 and ΔS^0 are the standard enthalpy and entropy of hydride formation at pressure p^0, R is the universal gas constant and T is the temperature.

In contrast to metal and complex hydrides, the storage capacity of sorbents (e.g. nanoporous materials) is typically expressed as gravimetric (wt%), considering both the mass of the sorbent and the up-taken hydrogen, or volumetric (vol%), related to the volume occupied by the solid, while the amount of hydrogen stored in the materials can be expressed in terms of total, absolute, excess storage capacity or net storage capacity [113].

With the gravimetric methods, which are more convenient for measurements not too far from room temperature, hydrogen uptake is determined by monitoring, with ultrasensitive microbalances, the evolution of a material's weight due to H-sorption, when it is exposed to a certain gas pressure under isothermal conditions. The most widely used method is the manometric, which is advantageous for measurements at cryogenic temperatures, and is based on monitoring gas pressure changes when dosing between calibrated constant volumes, at fixed temperature. The H_2 sorption capacity obtained in this case refers to excess adsorption, defined as the difference between the quantity of hydrogen gas stored at temperature, T, and pressure, p, in a volume containing the adsorbent and the quantity that would be stored under the same conditions in the absence of gas–solid interactions [112,114]. In order to deduce the excess hydrogen adsorption, the volume of non-adsorbed gas in the system is typically measured with helium which is assumed to be a non-adsorbing gas [115]. The absolute adsorption can be then derived considering that the amount of gas adsorbed on a
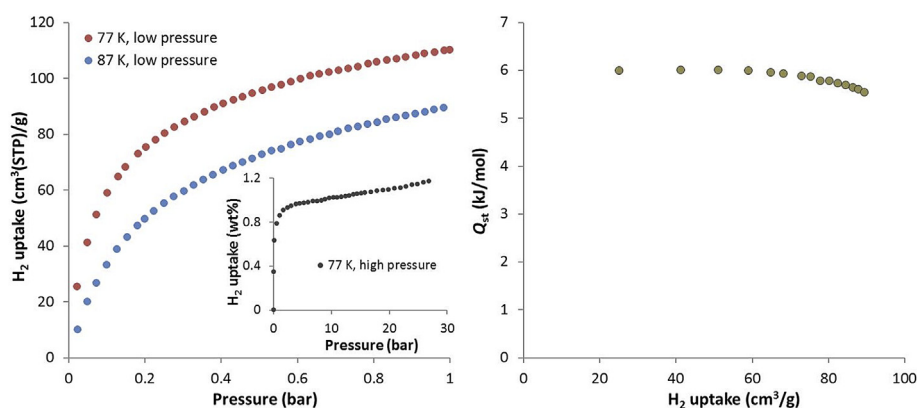
Fig. 6 – Left: High and low pressure H_2 adsorption isotherms at 77 K and 87 K of a high surface area, ultramicroporous magnesium formate. Right: H_2 isosteric heat of adsorption as a function of surface coverage.

sample is expressed as the total amount of gas introduced in the sample cell minus the free molecules in the gas phase [116]. This conversion is however based on critical assumptions that might affect the reliability of the obtained results. In this context, critical factors are the determination of "uncertain" quantities such as the volume (for manometric measurements) and the density (for gravimetric measurements) of the adsorbed phase, also as a function of pressure. Fig. 6, left shows high and low pressure H_2 adsorption isotherms measured manometrically using a PCTPro-200 (Setaram) and an Autosorb 1-MP (Quantachrome) system, respectively, at 77 K and 87 K for a high surface area, ultramicroporous magnesium formate [117]. The low pressure measurements at different temperatures allowed to calculate the corresponding isosteric heat of adsorption, Q_{st}, using the Clausius–Clapeyron equation (Fig. 6, right).

It is remarkable, that the same thermodynamic approach of extracting the isosteric heats of adsorption can be applied to occupancies of guest molecules refined from *in situ* diffraction experiments carried either in isobaric or isothermal modes [73]. In the former case, an interpolation of the data should be used for two experiments carried out at sufficiently different pressures. This approach offers the advantage of a simultaneous microscopic characterization of the guest location inside the pores. The main restriction is imposed on this technique by the possibility to locate reliably the guest, thus limiting the studies to the relatively small-pore systems with pore sizes below approximately 10 Å.

Solid state hydrides and *in situ* X-ray diffraction using synchrotron radiation

X-ray diffraction is a superior technique for structural characterization of crystalline matter strongly accelerated by access to intense, well-collimated photon beams from synchrotron X-ray sources. These high intensity sources have allowed development of *in situ* real-time techniques for a number of purposes, e.g. synchrotron radiation powder X-ray diffraction (SR-PXD) [118]. Real-time studies of solid–solid or solid–gas reactions at elevated pressures and temperatures in

different gas atmospheres are of particular interest for development of new SSHS materials and may simultaneously provide structural, chemical and physical properties as a function of pressure, temperature and/or time at different length scales, *i.e.* nanoscale structural data and bulk [118–121].

Metal borohydrides have attracted significant attention due to high hydrogen densities, but the conditions for hydrogen release and uptake need to be improved3 [122,123]. One such systems is the lithium potassium borohydride system, $LiBH_4–KBH_4$, where a phase diagram illustrates the low eutectic melting point of the composition $0.725LiBH_4–0.275KBH_4$, T_{melt} ~105 °C [124]. A bimetallic borohydride $LiK(BH_4)_2$ also exists in this system, which dissociates to the monometallic borohydrides at ~95 °C [124,125]. To distinguish the effect of grinding or manual mixing from the effect of thermal treatment on the formation of $LiK(BH_4)_2$, PXD studies were conducted. A sample of $0.5LiBH_4 – 0.5KBH_4$ was ground manually, placed in a borosilicate capillary, melted while in the capillary and then crushed manually before being placed in a new capillary for further analysis. The PXD analysis revealed the presence of the $LiK(BH_4)_2$ in two samples after grinding. These results concluded that heat treatment was not responsible for the formation of $LiK(BH_4)_2$, which was in contrast to previous investigations [124,125]. Analysis of the unit cell volumes of $LiBH_4$, KBH_4 and $LiK(BH_4)_2$ in the temperature range 25–90 °C using *in situ* SR-PXD data indicate that formation of the bimetallic borohydride is facilitated by a more dense packing as compared to the reactants. The smaller volume of $LiK(BH_4)_2$ compared to the added volume of $LiBH_4$ and KBH_4 reveal a more dense $LiK(BH_4)_2$ structure, which indicates that $LiK(BH_4)_2$ is likely stabilized by pressure and not heat treatment leading to thermal expansion [124] indicating that $LiK(BH_4)_2$ may be considered metastable and its formation is pressure induced. Thus, in general, mechanochemistry and manual grinding may facilitate formation of new compounds, with a higher packing density compared to the reactants [15].

Another example of benefit of using synchrotron radiation for powder diffraction is the solvent-based synthesis and
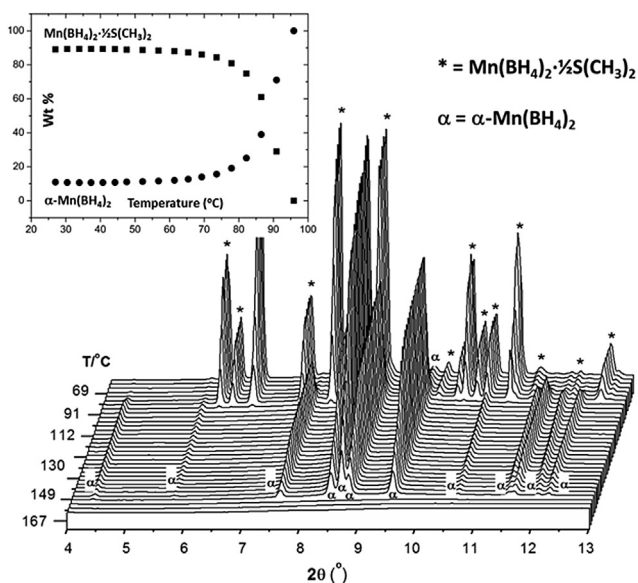
Fig. 7 — In situ SR-PXD measured from room temperature to 200 °C of Mn(BH₄)₂·½S(CH₃)₂ (λ = 0.696713 Å, p(Ar) = 1 bar). Inset: Integrated intensities (wt%) of Mn(BH₄)₂·½S(CH₃)₂ and α-Mn(BH₄)₂ as a function of temperature. Filled circles: α-Mn(BH₄)₂, filled squares: Mn(BH₄)₂·½S(CH₃)₂.

characterization of α-Mn(BH₄)₂ and a new nanoporous polymorph of manganese borohydride, γ-Mn(BH₄)₂, via a new solvate precursor, Mn(BH₄)₂·½S(CH₃)₂ [54]. The new polymorph, γ-Mn(BH₄)₂, is isostructural to the zeolite-like compound, γ-Mg(BH₄)₂, also with a 3D network of pores (diameter > 6.0 Å) in this structure. The solvate, Mn(BH₄)₂·½S(CH₃)₂, is also isostructural to the magnesium analog of Mg(BH₄)₂·½S(CH₃)₂. In fact, interestingly, a new polymorph of Mg(BH₄)₂, denoted by ζ-Mg(BH₄)₂ is also isostructrual to α-Mn(BH₄)₂. Temperature dependent in situ SR-PXD showed that Mn(BH₄)₂·½S(CH₃)₂ transforms directly to α-Mn(BH₄)₂ in the temperature range 70—95 °C (Fig. 7) while losing the solvated Dimethyl sulfide. Thermal analysis revealed decomposition of Mn(BH₄)₂ at 160 °C and a mass loss of 14.8 wt%, which is a mixture of diborane and hydrogen (ρ_m(Mn(BH₄)₂) = 9.5 wt% H₂).

An excellent recent example of using in situ diffraction to explore the mechanism of hydrogenation is made for the VO₂-H₂ system [126]. The synchrotron and neutron diffraction studies allowed to map out the structural phase diagram as a function of temperature and hydrogen content, to clarify the crystal structures and the physical basis of the related metal-insulator transitions.

Hydride thin films and ion beam analysis

Among the different nanostructures, hydride thin films are frequently investigated because of their relatively ease of synthesis and their low reactivity. During the H-sorption processes, thin films are excellent materials to systematically investigate the influence of microstructure (crystallite size,

strain) and surface states (presence of oxides, hydroxides or catalysts). The use of thin films also extends beyond SSHS media as the utilization of metallic films as hydrogen sensors and/or switchable mirrors becomes attractive for other applications.

The characterization of hydride thin films is usually performed by standard bulk techniques (e.g. X-ray Diffraction, Raman Spectroscopy and Electron Microscopy). However, extensive and thorough characterization can only be achieved with specific techniques (e.g. optical measurements, surface spectroscopies) that consider film morphology. These methods are widely used but many of them are not able to offer compositional analysis of the film and they are extremely surface sensitive or even sample destructive techniques.

In this context, Ion beam Analysis (IBA) is a set of characterization techniques that can easily cater for thin film samples as a quasi-non-destructive method for the near surface analysis of solids (~nm to ~μm) [127]. Moreover, they are fast, sensitive, quantitative and multi-elemental providing a detailed compositional depth profile of the films. In this technique, the sample is bombarded with ions having energies in the MeV-range (typically 0.5—4 MeV). The different events (X-rays, γ-rays and charged particles) emitted during the ion—target interaction provide information about the sample composition and determine the technique used. In particular, RBS-ERDA (Rutherford Back Scattering Spectrometry-Elastic Recoil Detection Analysis) are two complementary techniques to obtain depth profiles of heavier and lighter elements with the probe ion (usually He⁺) where a compositional map of the hydrogenated films can be obtained.

The RBS has recently been used to investigate the thermal decomposition of non-catalyzed MgH₂ [128] and Pd-capped MgH₂ films [129] providing new insights on the role of different interfaces on the desorption mechanism. To this aim, RBS and ERDA measurements were carried out at different stages of the hydrogen desorption process. For example, Fig. 8 a and b show the compositional depth profile of a hydrogenated and dehydrogenated Mg—Pd film, respectively. The hydrogenated film (~370 nm) exhibits a constant hydrogen concentration along the film depth with a ratio of H/Mg = 1.7 ± 0.1 indicating that film is fully hydrogenated. In addition, the Pd-layer on the Mg-film surface is also observed as well as the aluminum substrate (dashed region). Other elements such as oxygen can also be detected and this highlights the advantages of this method. The desorbed hydride film at 200 °C (Fig. 8b) shows a decrease in thickness (~300 nm) with no significant amount of hydrogen detected along the film. This result also shows that a Mg—Pd alloy is produced at the surface since the temperature is elevated enough to desorb the hydrogen from the film. Formation of this interface seems to be key to control the desorption mechanism.

Reactive hydride composite system and simultaneous thermal analysis techniques

Lightweight complex hydride systems including borohydrides and amides are advantageous due to high hydrogen capacities. New combinations of hydride materials can be tailored to specific operating pressures and temperatures as part of an
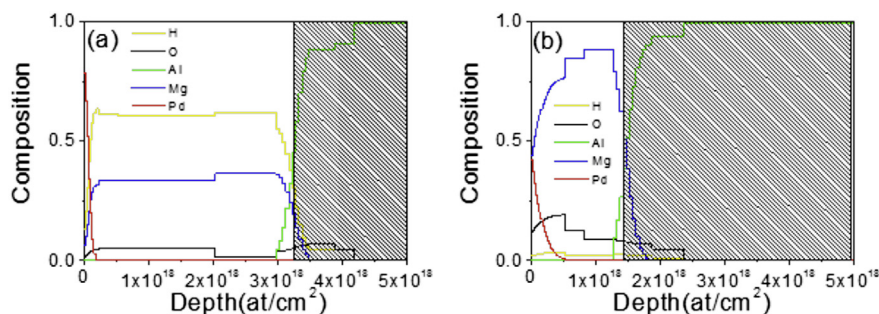
Fig. 8 – Depth profile of a hydrogenated (a) and dehydrogenated (b) Pd-capped Mg film. He$^+$ ions with energy of 2.6 MeV were used. Analysis of the ERDA and RBS results were performed with RBX software [130]. Dashed regions represent the aluminum substrate.

energy storage system coupled with renewable energy. High hydrogen content composites such as boron and nitrogen containing compounds are of increasing importance as combinations of hydrides have improved properties when compared to the individual components. One such reactive hydride composite (RHC) is the $LiBH_4$–MgH_2 system that is fully reversible at lower enthalpies than each individual compound [131,132]. It is important to measure accurately thermodynamic data such as reaction enthalpies as well as reaction kinetic information such as activation energies of reactive hydride composite systems and these can be obtained using thermal analysis techniques.

Thermal analysis, including differential scanning calorimetry (DSC) and differential thermal analysis (DTA), measures the difference in heat flow due to thermal transitions of a sample and a reference. In the case of H-storage materials, hydrogen absorption is usually an exothermic reaction and hydrogen desorption is an endothermic reaction. The more stable the bonds between the metal and the hydrogen, the higher the enthalpy or energy needed for either absorption or desorption to occur. The DSC keeps the temperatures of the sample and of the reference material identical and measures the difference in applied power, while DTA applies the same heating power and measures the temperature difference, from which the heat flow is determined. The integral of the heat flow curve recorded in the course of a transition gives the heat of transition. This technique enables the measurement of the temperature dependence of specific heats, enthalpies of reaction and can also be used to give kinetic information such as activation energies from the Kissinger method [133,134]. In order to account for the sensitive nature of hydride materials to oxygen or moisture, DTA or DSC instrumentation can be installed and fully operated in an inert atmosphere glovebox without any compromise to the technique. This reduces the risk of reaction with O_2 or H_2O during heating ensuring that contamination is low during measurements.

Further, DTA analysis can be coupled with complementary measuring techniques such as thermogravimetic analysis (TGA) and mass spectrometry (MS) (Fig. 9) to simultaneously measure changes in weight of the sample and also identify any gases that may be released during the desorption reaction [135,136]. TGA uses a series of microbalances that can accurately measure a decrease in weight on the milligram scale during the same temperature program as the DTA. Similarly,
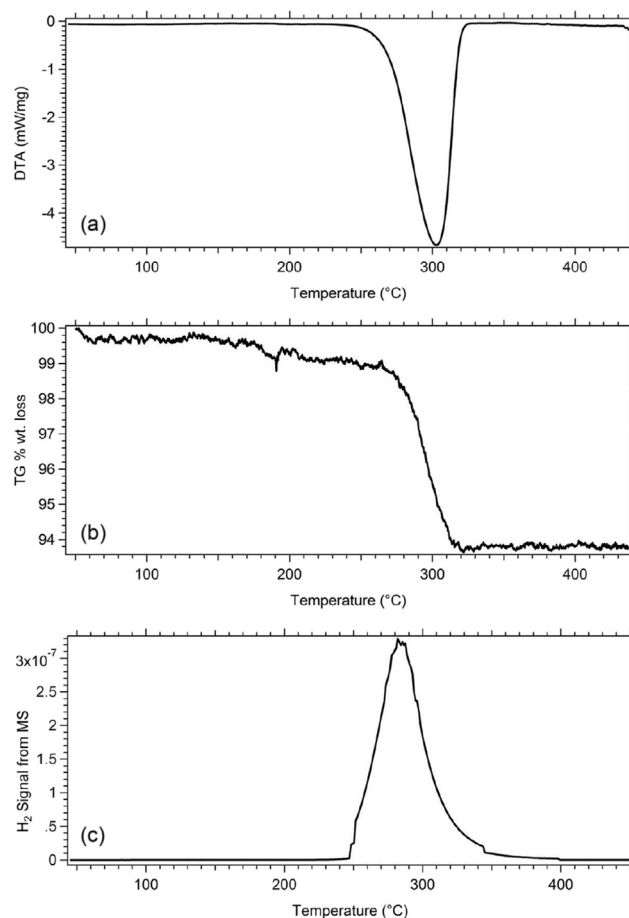
Fig. 9 – Thermal analysis from the complex hydride Mg_2FeH_6 upon heating at 5 °C/min: (a) Differential Thermal Analysis (DTA); (b) Thermogravimetric Analysis (TGA); (c) H_2 detected from mass spectroscopy (MS) [135].

the MS can detect the release of not only H_2 but also gases such as B_2H_6 and NH_3, which may be released during RHC desorption. The differential techniques (DSC and DTA) together with the TGA and MS are able to determine thermal transitions at specific temperatures and also show whether the reactions occur in single or multiple steps as shown in Fig. 9.

Preparation of hydrogen storage materials for tanks

Selection of appropriate hydrogen storage materials to be used in tank systems can be achieved through the various characterization techniques described in the previous sections. However, once these materials are inside the tank further analysis of the behavior needs to be fulfilled. Heat management and gas transport are two important aspects to consider during tank design for hydrogen storage. Previous studies have shown that material in the form of powder inside tanks could be detrimental for its performance [137,138]. Hydride powders tend to pack and sinter during repeated H-sorption cycles causing a reduction in hydrogen system capacity and slower gas–solid reaction kinetics. One solution to address these issues is the compaction of the powder into pellets prior to placement in the tank [137]. The use of compacted powders instead of free powders provides minimal risk of contamination (oxygen or moisture) to the hydrides, facilitates the charging of the material in the tank by it improving heat conduction and improving gas transport through the system [138–141]. With the improvement of compacted powder, the material inside the tanks would have constant and stable hydrogen uptake and release properties.

In addition to compaction, the introduction of carbon-based materials can improve the performance of the materials inside a tank. In the case of Magnesium-based systems, it was reported that the use of carbon-based materials such as carbon nanofibers and expanded natural graphite (ENG), could improve the stability [141–144]. It was reported that ENG stratifies along a direction perpendicular to the axis of compaction allowing the gas to diffuse in the material therefore increasing the mechanical stability of the pellets. However, the formation of cracks in the compacted systems was observed after cycling under hydrogen pressure. These cracks appear in zones areas where the material appears to be heterogeneous [145]. For this reason, the effect of the compaction pressure on the mechanical stability of the pellets under cycling was studied. The compaction pressure positively affects the characteristics of the pellets and it was observed that the higher the compaction pressure the lower the variation of dimensions of the pellets with cycling [31].

The preparation of the pellets of ball milled MgH_2 with Nb_2O_5 as a catalyst was implemented by coating with nanosized metals (for example Cu, Al, Cr) or oxides. Hydrogen capacity and kinetics of these systems showed good stability in that there was no significant change over 50 cycles of H-sorption at 310 °C and 8 and 1.2 bar respectively. The pellet showed drastically increased structural stability compared to the same material without the nanometric additives. Fig. 10 shows a SEM image of the pellet where the thin Al layer on the surface and the Nb_2O_5 (white spots) are clearly visible.

Neutron radiography for solid state storage tank design and performance

The final approach towards application of solid state materials in a storage system is the design and performance of the tank itself, together with the characterization of the enclosed material. There are several aspects associated with tank design including theoretical modeling and simulations based on tank geometries and materials [146], heat transfer and coupling with units such as an electrolyzer or fuel cell. To be more specific when it comes to the design of the storage tank, it is necessary to take into account a number of parameters such as hull material, tank diameter and tube arrangement to optimize hydrogen transport, intrinsic kinetics and heat transfer to and from the material [146]. To investigate further the performance of both the tank and the material inside the tank it is necessary to develop special characterization methods such as neutron radiography.

In situ neutron radiography is a technique that allows for time resolved hydrogen distribution in metal hydride systems
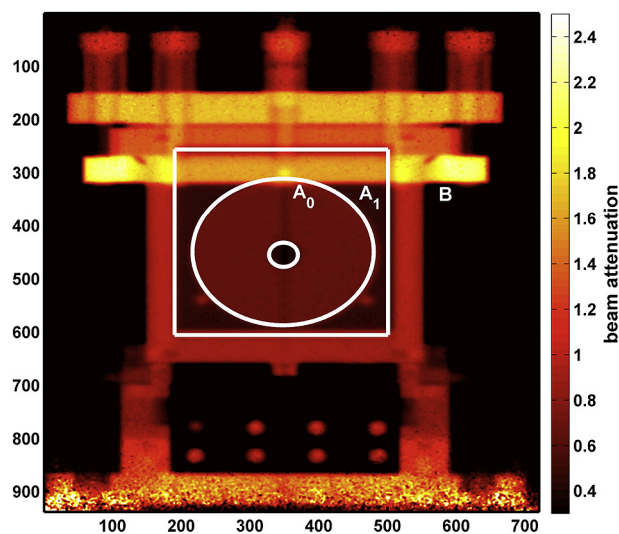
Fig. 11 – Processed radiography of the investigated metal hydride material (147.5 g) inside a tank made of aluminum. The image is normalized by the flat field and corrected for the dark image. Additionally, a negative logarithm is applied to derive the distribution of the neutron beam attenuation. The area within the circle is the projected volume containing the metal hydride material, denoted by A_0. In the remaining area the attenuation is time independent, it is denoted by B. Area A_1 in the lower part corresponds to free volume inside the aluminum tank [146].
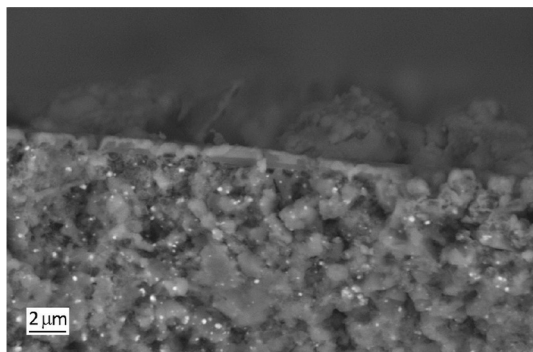

Fig. 10 – SEM image of a fracture of the pellet prepared by ball milling MgH_2 with 5wt% Nb_2O_5, 5wt% ENG and coated with Al, after 50 cycles at 310 °C under H_2 pressure of 8 bar (absorption) and 1.2 bar (desorption).

within a storage tank especially designed for the technique [146]. Due to the strong hydrogen–neutron interaction cross-section it is possible to quantitatively analyze and spatially resolve the hydrogen content that is absorbed by the metal hydride material. A method was developed recently by Börries et al. [147] to investigate and clarify the influence of sample scattering on the measured intensity field, which was shown exemplary for two different tank hull materials, aluminum and stainless steel. Fig. 11 shows a processed radiography image of a hydride material inside a tank made of aluminum. Using a fission neutron spectrum, it was demonstrated that it exists a strong linear correlation between the attenuation by hydrogen and the amount of hydrogen absorbed in a sodium alanate system, which was referred to as a model material. It was concluded that quantitative *in situ* neutron imaging is a valid technique for investigation of hydride materials in general [147]. This method can therefore lead the way in terms of quantitative material analysis inside scaled-up metal hydride systems, greatly contributing to the optimization of future storage tanks in terms of application.

Computational methods for novel materials and systems for H_2 storage

Novel approaches in computational materials design for efficient hydrogen storage

Many interesting mixed or doped compounds have been proposed and experimental verified, often based on chemical intuition by mixing similar elements. Through these human-guided (also computational) experiments various materials have been continuously improved in small steps. However, the incremental change of parameters is very time-consuming both using computational techniques, during synthesis and characterization, and the materials properties are generally only modified slightly. Instead of only testing slight deviations from what is known to work, large high-throughput screening studies test many different combinations substituting elements systematically, possibly resulting in superior materials [148–150]. However, due to the fact that chemical knowledge is often not included *a priori*, many of the suggested mixtures would not be stable, and possibly decompose upon cycling. Using computational screening is therefore often a useful tool to sort away mixtures, which for sure are not interesting, as it is faster, possibly cheaper, and does not generate any chemical waste.

Given the computational speed, it is generally beneficial to be inclusive when searching for new mixtures, and limit or avoid exclusion of specific material combinations prior to a study, e.g. due to cost or toxicity. Because of this, the investigated configuration spaces can easily contain many thousand candidates, which should be tested computationally. Despite the fact that improved methods have been developed and the computational power continues to increase, it is generally not feasible to study all materials in great detail, e.g. to identify the lowest energy crystal structures. One approach, which can be followed to lower the computational cost, is template based screening, where the atomic ordering is (partially) fixed in representative crystal structures, which is

significantly faster than allowing full relaxation of all structures [148,149]. Limiting the possible symmetries is to some extent at the expense of the obtainable accuracy, but it will often be possible to investigate trends and identify promising and stable mixtures, which subsequently can be studied in detail. If so, it is also important to have an inclusive selection approach allowing slightly unstable structures for further studies, as they might become stable upon full relaxation.

As an alternative to brute-force high-throughput screening studying every candidate in a large search space, different methods are available to reduce the number of candidates to test. One very useful method are the biologically inspired genetic algorithms (GAs) based on natural, *Darwinistic*, selection favoring the survival of the fittest species [148,149,151,152]. The GAs can be very useful to guide structural optimization of complex systems containing many atoms, as for example carbon allotropes [153] and nanoparticles [154,155], which is a computationally challenging task, as the potential energy surfaces contain an enormous amount of local minima. Ordinary local optimization methods are often very slowly converging and would often not locate the global optimum, which is easier with GAs because it can make big "jumps" by combining important structural units. Combining the methods to create a GA method allowing subsequent structural optimization of the suggested candidates using gradient-based methods can often be advantageous.

The basic idea in GAs is to maintain a *population* of the best materials, which is initiated using a number of randomly selected compositions (Fig. 12). From the population, new *generations* are created using the genetic information from the current *parent* structures and various *operators*. In general, two types of operators are available to generate new *offspring*: the *crossover* taking one part from one parent and *mating* it with a part from another, allowing the identification and reuse of important building blocks; and to reduce the risk of being trapped on local minima in configuration space, *mutation* operators, which make random changes, are very important. The most *fit* of the generated offspring are kept in the population to generate further offspring in subsequent generations. The *fitness* of a structure determines where the search should progress, and can be defined as a function, for example the gravimetric hydrogen density (wt%), release temperatures, price, toxicity and stability of the mixture. Often it is advantageous to define a more simple *fitness function* containing only one or a few parameters as for example the wt%, and then in addition apply some *selection rules* determining, which structures are not allowed in the population, e.g. to deselect expensive or unstable mixtures.

One class of materials, which have been investigated using GAs are the mixed metal halide ammines. The pure metal halide ammines are very well known, and many metal/halide combinations are known to have stable ammine phases [156]. A challenge for the pure metal halides is however that they generally show multi-step releases over broad temperature intervals [157]. Furthermore, the release temperatures are often too high resulting in low total efficiency, as too much energy has to be supplied to release the ammonia. Very large configuration search spaces have been investigated, containing up to 100,000 structures mixing alkaline earth, 3d and 4d metals with different halides in a unit cell with up to 8 metal
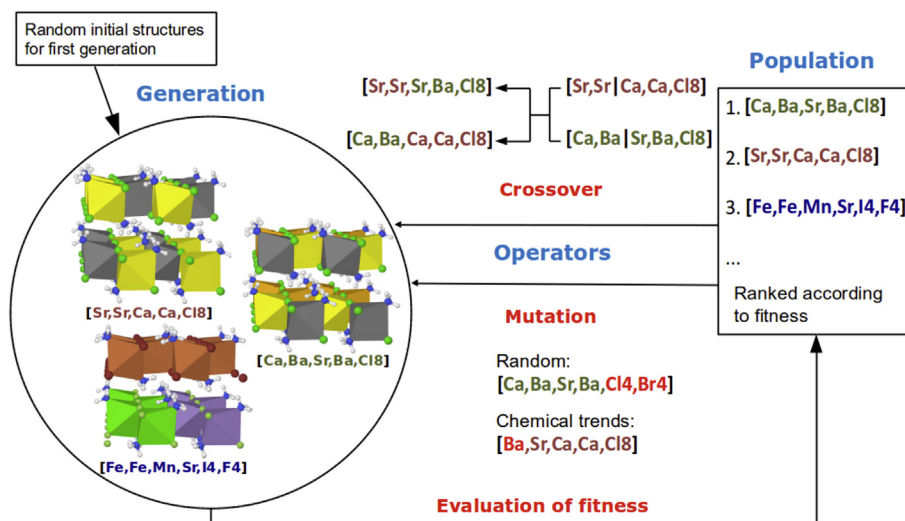
Fig. 12 – Illustration of a genetic algorithm searching for optimized material mixtures using templates. The individual candidates are encoded as vectors describing the contained metals and their position in the templates. Using various operators, the algorithm generates new trial candidates by using the information from one or more parents.

atoms, resulting in a lowest "dopant" concentration of 12.5% [149]. Using the genetic algorithms, Jensen et al. demonstrated that the global optimum for the mixed hexa ammines in the defined search space of more than 54,000 structures, could be identified consistently by calculating less than 2% of the candidates [148]. By using the GAs not only the global optimum structure was found, but also a population containing many interesting mixtures was identified. This is very beneficial compared to only identifying the global optimum, taking into account that the study was template-based, which as mentioned could introduce some inaccuracies.

In a subsequent study by the same group, the complexity was further increased by including many possible intermediate ammine phases [149]. The fitness was defined to search for materials releasing the ammonia between 0 and 100 °C, which is a temperature range suitable for e.g. system integration with low-temperature polymer electrolyte membrane fuel cells (PEMFC). The efficiency of the implemented algorithm was verified by three trial runs capable of finding the same optimal mixtures starting from different random populations, testing <5% of the candidates in a search space containing more than 100,000 structural combinations. In Fig. 13, all the
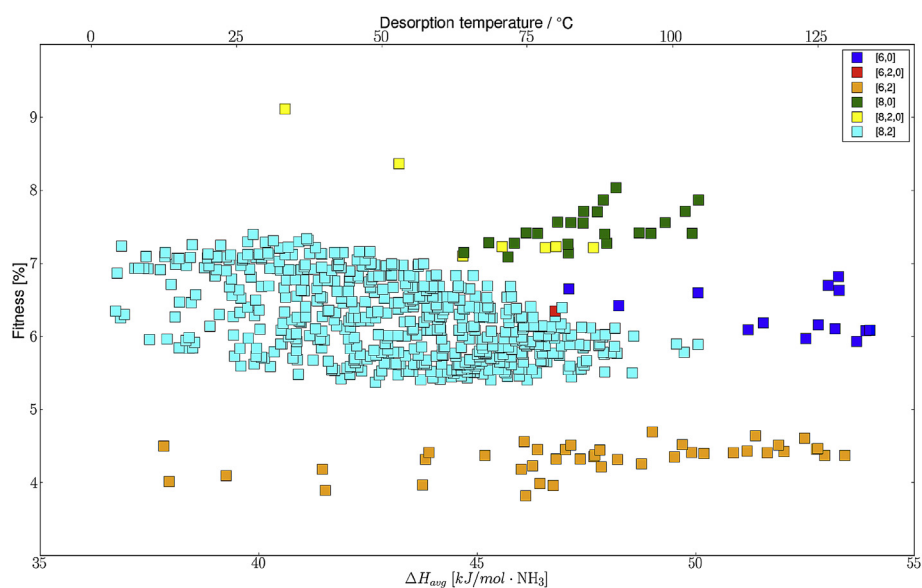

Fig. 13 – Visited parts of the search space, showing that different reactions are grouped in bands. The legends and coloring show the predicted observed phases, where 8 signifies octa ammine, 6 hexa ammine, 2 di ammine, and 0 the empty salt. Reprinted from Ref. [149] with permission. Copyright 2015, American Chemical Society.

stable mixtures releasing the ammonia in this temperature interval are grouped according to the release patterns. As can be seen from the figure, the two best structures, which are found by all three runs, are decoupled from the other investigated structures, proving the algorithm's ability to identify structures in narrow regions of the phase space. The two best structures are special in that they display a multistep release within the temperature interval, which is only seen for a very limited number of structures in the searches (many materials do have a multistep release but with some of the releases at too low or high temperatures). The remaining structures seem to be more correlated, also proving the algorithm's success to find the optimal solution in a small subset. Some of the best candidates were already confirmed experimentally, and others offered a record high, accessible hydrogen capacity exceeding 9 wt%. Among the identified materials is the first known high-capacity ternary metal halide ammine, $Ba_{0.5}Sr_{0.375}Ca_{0.125}(NH_3)_8Cl_2$, which was subsequently synthesized and tested, thereby confirming the ammonia storage properties.

Functionalization effect and elemental substitution

Functionalized 2D materials (graphane, silicene and silicane)
Systematic DFT based electronic structure investigation [158–161] has been carried out for pristine and hydrogenated silicene and graphane functionalized with a series of alkali and alkaline earth metals (Li, Na, K, Be, Mg and Ca). It was found out that Li-functionalized graphane sheets could attain the storage capacity of 3.23 wt% with concentration of Li doping as low as 5.56%. Ca-functionalized graphane also shows a reasonable H-storage capacity of 6.0 wt% with 11.10% doping concentration of Ca adatoms. For silicene, Li and Na have been found as most prominent dopant adatoms adsorbing four H_2 molecules in their corresponding vicinity. The storage capacities of Li- and Na-functionalized silicene are 7.75 wt% and 6.90 wt% respectively, with the adsorption energy in the range suitable for practical H-storage applications. In the case of hydrogenated silicene or silicane, the binding energies for Li and Na functionalization are 0.63 and 0.55 eV/atom, which are greater than their respective bulk cohesive energies. This rules out the possibility of adatoms aggregation on surface. The H-storage capacities for Li and Na are 6.30 wt% and 5.40 wt% respectively, which are the most efficient ones compared to the other adatoms to functionalize silicane.

The mechanism of hydrogen adsorption in molecular form on each solid state substrate in pristine and hydrogenated form have been investigated, finding that H_2 molecules are adsorbed on each adatoms stepwise in a one by one manner. Each H_2 molecule around the metal adatom is polarized while approaching to the adatom and adsorbed due to weak van der Waals forces along with the electrostatic interactions. The H_2 molecules attach vertically to the metal adatom in order to increase the H_2 storage capacity and simultaneously maintain the physisorption distance between them. This also leads to the spontaneous reduction of the unwanted repulsion between the H_2 molecules imposed by the polarization effect of the metal adatoms. The Bader charge analysis also reflects the interaction of the metal adatoms with the two-dimensional

sheet of graphane, silicene and silicane. The analysis predicts the charge transfer direction between the metal adatoms and the sheet. The bonding between the metal adatoms and the sheet has been expedited with the electron donation and simultaneous acquisition of a net positive charge to the metal adatoms. This efficient charge transfer also enhances the electrostatic interactions between the metal adatoms and the two-dimensional sheets.

Effects of doping and elemental substitution in 3D materials
It is experimentally well known that dopants and substitutional elements can have dramatic effects regarding e.g. the stability and kinetics of the release of hydrogen from a solid phase [162–164]. Using computational methods, one can easily exchange the elements in the crystal structure of a given material, and systematically search for materials compositions with improved properties. Due to the fact that doping is generally the result of a trace impurity element, introduced in a low concentration, quite big unit cells are often needed to describe the system. When studying solid materials, it is also difficult to study the effect of the position of the dopant(s) in the material, and periodic boundary conditions are in general imposed, resulting in materials with the dopants regularly distributed, which might not be experimentally observed. Because of these limitations, "real" dopant effects are normally not studied, as this would require vast computational resources. Most studies are instead focusing on studying the effect of mixing different elements in certain ratios, thereby allowing the study of trends and making it possible to identify important regimes that subsequently can be studied in details experimentally or computationally.

The latter approach was followed by Biliškov et al. to study the effect of partially exchanging Ni for either Ga or Al in $SmNi_5H_x$ [165,166]. In the combined experimental (XRD and hydrogen desorption) and computational (DFT) studies it was predicted that the intermetallics with Ga or Al substitutions would be thermodynamically stable. Furthermore, it was shown that the substitutions preferentially take place in a specific layer of the structure, and that the hexagonal P6/mmm space group is retained when substituting up to 50% of the Ni, in agreement with experiments. The absorption of hydrogen in different interstitial positions was studied, and the stabilities and H-storage capacities of the hydrides were found to depend on the substitutions. Especially the local coordination of the hydrogen atoms to the metals is important: hydrogen atoms prefer positions that are not coordinated with Ga or Al atoms. Using the gathered insight, the effect of substitution by other or multiple metals at a time can now be studied, and thereby it is possible to select only the most relevant candidates for experimental testing.

Complex hydrogen storage materials in the form of metal halide ammines are promising candidates for indirect hydrogen storage [167], due to high hydrogen densities [168], good cyclability and H-sorption kinetics [169,170]. Strontium chloride is one of the most studied metal halide ammines, allowing the storage of eight ammonia molecules coordinated to each metal atom giving 8.2% hydrogen by weight in $Sr(NH_3)_8Cl_2$ [170–172]. The major drawback with strontium chloride is however that the ammonia is released in two or three steps depending on the pressure and temperature,
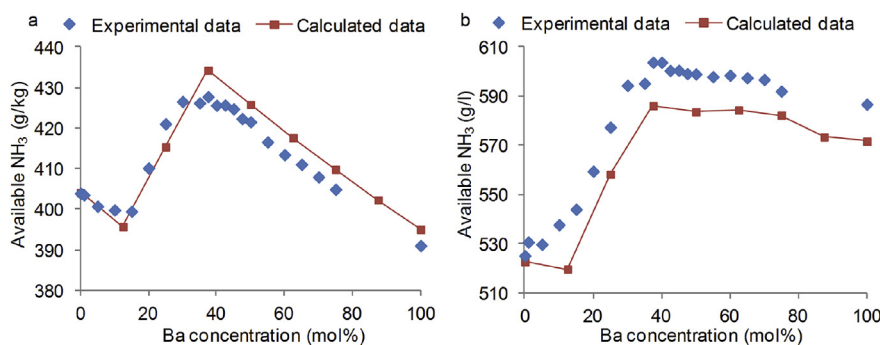
Fig. 14 – Usable ammonia densities of ammoniated $Ba_xSr_{(1-x)}Cl_2$. (a) Experimental and calculated usable gravimetric ammonia density as a function of Ba concentration. (b) Experimental and calculated usable volumetric ammonia density as a function of Ba content. Reprinted from Ref. [174] with permission. Copyright 2015, Elsevier.

bypassing a di and/or a mono ammine [171]. Furthermore, the last ammonia molecule is generally too strongly bound requiring higher temperatures for the release (>100 °C). $Ba(NH_3)_8Cl_2$ on the other hand do show a one-step release, but the ammine is not stable at room temperature. From van der Waals corrected DFT calculations (vdW-DF [173]) it was shown that solid solutions of $BaCl_2$ and $SrCl_2$ should show increased available storage capacities surpassing both of the pure salts [174]. Through synthesis and experimental tests, it was shown that mixtures with a Sr:Ba ratio of around 40:60 displayed an optimum capacity and a one-step release in excellent agreement with the theoretical predictions (Fig. 14). The mixed material show very high gravimetric and especially volumetric ammonia capacities, comparable to that of liquid ammonia, while maintaining safe handling due to a low vapor pressure at standard conditions. Using template based screening in larger screening studies it was also tested whether mixed metal halide ammines could be tuned to give a high available ammonia release in a desired temperature interval [148,149]. Through these studies, a wide range of candidates were identified, some of which might have been suggested from chemical intuition, e.g. $Ba_{0.5}Sr_{0.375-}$ $Ca_{0.125}(NH_3)_8Cl_2$, whereas others as e.g. $Ti_{0.25}Cu_{0.5}Mg_{0.25}(NH_3)_6Cl_2$ would have not been proposed.

Ab initio calculations for Mg based metal hydrides

MgH_2 is an interesting candidate for SSHS due to high gravimetric capacity and low price, but has the major drawback that the hydride is too stable, resulting in high release temperatures and slow kinetics [175]. To improve the material's hydrogen release properties, "doping" with various elements was extensively investigated experimentally and computationally. However, due to the mentioned problems with large unit cells, the dopant concentration has been at least 6.25% [150,176–179]. DFT was used to study how dopants and strain affect the electronic structure and the density of states (DOS), which have been correlated with H-sorption energies [177–179]. Through the computational studies, it has been possible to describe the catalytic effect resulting from the destabilization of the crystal structure as a result of the

substitutions. Another information that can be gained from the structural relaxations, are the volumetric hydrogen storage capacities change due to the dopants. H-sorption kinetics were not included in the studies, because they require the use of computationally very expensive methods.

An interesting study by Giusepponi et al. investigated dopant effects for low concentration dopants, using DFT to study how Fe dopants catalyze the hydrogen diffusion in the magnesium hydride [180]. In the study, it was investigated how dopants destabilize the materials by altering the metal-hydrogen bonding at the $Mg–MgH_2$ interface. It was found that doping with a few percent of Fe, Co, Ni, Nb and Pd is energetically favored. Moreover, as found in experiments, the dopant concentration is highest near the interface, catalyzing the release of hydrogen. The major part of the work is devoted to an *ab initio* Car–Parrinello molecular dynamics (CPMD) study of the hydrogen release at elevated temperatures for the Fe-doped system, which was previously shown to perform well [181]. Due to the size of the system (low dopant concentration) and the general challenges with MD simulations requiring sampling of an enormous amount of atomic configurations, the computational methods have to be carefully
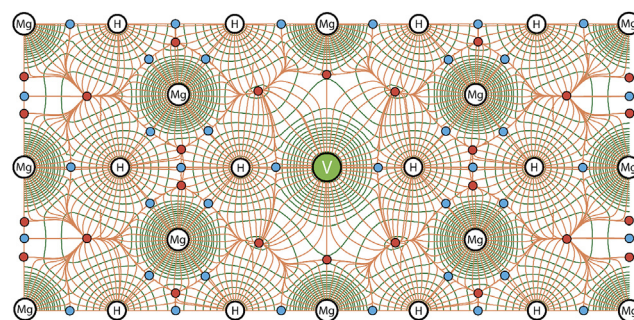

Fig. 15 – Charge density (green) and its gradient (red) field in the MgH_2-V (1–10) plane. Blue and red filled circles designate positions of bonding and ring critical points, respectively. (For interpretation of the references to color in this figure legend, the reader is referred to the web version of this article.)

chosen to ensure an acceptable accuracy within a limited time frame. In this study, the simple local density approximation (LDA) and pseudopotential approach with a limited number of valence electrons were used to lower the computational cost. By observing the mobility of the hydrogen atoms at different temperatures, a lowering of the desorption temperature to 500 K is observed compared to the system without metallic doping that shows no desorption below 600 K. This fundamental study of the highly investigated MgH_2 and the agreement with experiments shows that it is possible to accurately study the dynamics of solid materials using DFT, opening up for further investigation and improved understanding of reaction mechanisms for related materials.

Ab initio electronic structure calculations of the $Mg_{15}TMH_{32}$ (TM - transition metals) systems for the complete 3d TM series were performed by Paskaš Mamula et al. [150]. The bonding and the mechanism of MgH_2 destabilization by TM metals were investigated using the "atoms in molecules" (AIM) Bader's charge density topology analysis (Fig. 15). The acquired trends show that, along the 3d TMs series, different kinds of bonding to nearest hydrogen atoms are accomplished, that in general weaken related Mg–H bonds and destabilize the surrounding MgH_2 matrix. The specifics of bonding critical points arrangement, the charge density in these points and the value and sign of its Laplacian indicate the rising of covalence-to-ionic ratio in TM-H bonding along, with the trend being reversed at the end of the 3d TM series. The bonding strength and bond lengths obey the same trend, which can be explained in terms of alternate filling of bonding, non-bonding and anti-bonding states. Effect of TM doping is nevertheless localized to a few neighbor shells only, so the influence TMs have on hydrogen desorption process cannot be fully ascribed to electronic effects [150].

Further, ab initio calculations were used to investigate hydrogen desorption from the (110) surface of β-MgH_2. The H-desorption was reproduced as a consecutive release of the four two-fold bonded H atoms from the surface. It was shown that decrease in number of surface H atoms lowers the H-desorption energy in each desorption step and that both the H–H and the Mg–H interatomic interactions have an effect on the H-desorption process. The hydrogen vacancy formation energy in the first three sub-surface layers also exhibits a pronounced dependence on concentration. One can conclude that the tendency of the MgH_2 (110) surface to preserve a maximum possible surface H concentration in its most stable configuration is the limiting factor for the H-desorption kinetics. The obtained results allow to determine the preferred paths of surface and sub-surface H-diffusion for a wide range of H concentrations and the principal features of the MgH_2 dehydrogenation process, at least for the H-rich region [182].

Effect of external strain, anisotropy and nano-confinement in nanostructures

Effect in 2D nanostructures

One can also increase the efficiency of a solid-state matrix by applying an external strain on it, which leads to the functionalization stability of the material. The strain induced stabilization of the Li adatom on graphane and Mg adatom on pristine and hydrogenated silicene or silicane have been studied. The two-dimensional sheets are also confirmed to be stable under external mechanical strain [183,184]. This has been validated by the experimental correspondence of applying external strain up to 15%, and the sheets were found to lie within their elastic limits under such high strain. The electronic structure calculations were employed already to study the effect of external biaxial asymmetric strain (7.5% and 10% along X and Y direction) on Li-functionalized graphane. The external strain increases the stability of Li-doped graphane and uniformly distributes the adatoms on the sheet. Both sides of the sheet can adsorb maximum four H_2 molecules with the corresponding storage capacity of 12.12 wt %.

In the case of pristine and hydrogenated silicene or silicane, it was found that Mg-functionalized sheets do not have high storage capacity. However, under the biaxial strain up to 10% on both sheets, the Mg adatom can be attached with maximum six H_2 molecules with the corresponding storage capacity of 8.10% and 7.95% for silicene and silicane respectively. The external strain increases the binding energy of Mg to silicene and silicane sheets compared to the corresponding bulk cohesive energies. This removes the possibility of clustering of Mg adatoms on silicene and silicane sheets, which is one of the hindrances behind decreasing the hydrogen storage capacity. The larger binding energy significantly decreases the surface to adsorbate distance and increases the Mg–Mg bond lengths, thus leading to uniform distribution of the adatoms on the surfaces rather than cluster formation.

Effect in 3D nanostructures

As discussed earlier, computational studies are often focusing on the atomic details, which can result in macroscopic effects. Ahuja et al. have for example studied the combined effect of strain and dopants resulting in improved desorption from magnesium hydride [177,179]. Applying a strain along the direction of Mg–H bond was found to bring down the dehydrogenation energies resulting from a direct weakening or lengthening of the Mg–H bond. Furthermore, addition of certain transition metals resulted in a higher volumetric capacity, due to a decrease of the equilibrium volumes.

Combining DFT calculations and in situ X-ray powder diffraction (XRPD), Johnsen et al. explained the anisotropic thermal expansion of $Sr(NH_3)_8Cl_2$ [172]. From the experiments, it was evident that the bonding distances between strontium and the eight coordinating ammonia molecules were not equal. Using DFT, the binding energies of the three different Sr–N bonds were analyzed, and it was found that one of the ammonia molecules was significantly easier to distort from the equilibrium bond distance. This loosely bound ammonia is oriented almost parallel to one crystal direction, resulting in an anisotropic expansion of the material upon heating, which could be described from the ground state properties, by estimating the expansion coefficients [185].

The decomposition of $LiBH_4$ takes place at temperatures above the melting point of $LiBH_4$, resulting in partial deactivation due to agglomeration of the reactive powders. Nano-confinement of metal borohydrides is a promising route for improvement of the poor kinetic and thermodynamic properties related to hydrogen storage [186,187]. Łodziana et al. have studied nanostructured $LiBH_4$ extensively and accurately

predicted the ^{11}B NMR chemical shifts [188,189]. The calculated NMR parameters provide detailed insight, at the atomic scale, into the properties of nanosized structures. More detailed models describing the nanoconfined borohydrides have also been suggested, giving some possible explanations of the observed decreased hydrogen capacity during cycling in carbon based materials [189,190].

Monolayer boron nitride (BN) and boron carbides (BC$_3$) sheet

The hexagonal boron nitride (h-BN) and boron carbide (BC$_3$) also emerged [191,192] as promising H-storage materials in the last years. The functionalization of Ni and Rh elements replacing nitrogen in BN sheets enhances the H-storage capacity. Additionally, an external electric field also increases the H-storage capacity by adsorbing three H_2 molecules with a gravimetric density 7.5 wt%. The electric field application in H-storage phenomena is also quite attractive because of the reversibility factor of H_2 release at the electric field removal time. It also provides a controlled tool for reversible H-storage and the energetics and kinetics of the systems can be tuned by tuning the applied electric field. Additionally, one does not need the complicated synthesis route to embed the metal ions under the electric field application and also the chance of those ions to be clustered during the simultaneous hydrogenation and dehydrogenation becomes less probable. The stabilities of the sheets do not get perturbed with constant H_2 uptake and release, and there is lower probability of getting poised with other gases. Tuning the suitable electric field strength can control the reversibility and kinetics of the sheet.

During the last years, the polylithiated species containing a large density of Li atoms were investigated experimentally and theoretically aiming at enhancing their hydrogen storage capacity. The polylithiated compounds CLi$_n$ (n = 3–5) and OLi$_m$ (m = 1–4) emerge as highly stabilized compounds with a strongly C–Li and O–Li polar bonds respectively. CLi$_4$ and OLi$_2$ compounds can bind to twelve and ten H_2 molecules individually. Therefore, functionalization of the two-dimensional sheets with such polylithiated species can increase the hydrogen storage capacity for practical applications. The h-BN sheet functionalized with CLi$_3$ and OLi$_2$ can adsorb up to three and four H_2 molecules leading respectively to 6.80 wt% and 6.11 wt% H-storage capacity, with reasonable adsorption energy range, which is important for practical H_2 storage at ambient conditions. It is worth to mention that all these polylithiated-functionalized sheets were checked for the dynamical stability at room temperature by phonon dispersion molecular dynamics simulations based on DFT based electronic structure formalism.

The polylithiated functionalized BC$_3$ monolayer sheet is also quite useful in terms of hydrogen storage capacity. It has been found that the storage capacity attains 9.83 wt% with feasible binding energy, while functionalized with CLi$_3$ and each Li binds to four H_2 molecules. In case of CLi$_4$ and OLi$_2$ functionalization, the hydrogen storage capacities are 11.80 wt% and 8.70 wt% respectively. The BC$_3$ sheet after functionalization with CLi$_3$, CLi$_4$ and OLi$_2$ has been examined from the dynamical stability perspective based on phonon dispersion and molecular dynamics study. The OLi$_2$

functionalization has been envisaged in case of hydrogenated graphene or graphane as well, where it shows 12.90 wt% of hydrogen storage capacity with each Li can hold up to three H_2 molecules at an instant. The polar nature of C–O and Li–O bonds are predicted from Bader charge analysis in the case of graphane and it is worth to mention here that OLi$_2$ are replacing the two hydrogen atoms of graphane [193,194] in order to avoid the cluster formation that can effect the reversibility of the hydrogen storage and release by the solid state matrix.

The number of Li atoms in polylithiated species is not really restricted to m = 1–4 (for OLi$_m$) and n = 3–5 (CLi$_n$). There are species containing higher number of Li indeed, but it has been seen that the average charge on Li decreases as the number increases due to the metallicity of the coordination shell. This leads to reducing the H_2 molecule adsorption by individual Li$^+$ ion through the electrostatic interactions. The partial change on each lithium should be maximum in order to attain the maximum possible H_2 storage capacity. In addition to this, the hyper-coordinated polylithiated species can also decrease the stability of the dopants on the two-dimensional nanostructures. It is worth to mention that the binding energies of CLi$_4$ an OLi$_2$ adsorbed on the top of C and B of BC$_3$ sheet are found to be the minimum energy configurations among all possibilities. The binding energies for CLi$_4$ and OLi$_2$ with BC$_3$ are higher than the individual dimerization energies of the both polylithiated species. This leads to the least possibility of cluster formation on BC$_3$ monolayer and prevails the uniform distribution of CLi$_4$ and OLi$_2$ over the BC$_3$ nanosheet. The formation of Li$^+$ ion arises due to the significant charge transfer from Li to C and O in the case of CLi$_4$ and OLi$_2$ because of the electronegativity difference and this favors the H_2 adsorption around Li$^+$ ion through the electrostatic and weak van der Waals interactions.

The importance of computational modeling

As highlighted by the presented examples, computational modeling of materials for solid state hydrogen storage has reached a level where it is now possible to accurately describe and predict the thermodynamic and structural properties, even for large configuration spaces. It has also become possible to explain a range of complex experimental observations, such as anisotropic thermal expansion or the fact that mixing known materials or doping with different elements can result in materials with optimized thermodynamics and kinetics. Even more important, it is now possible to use the computers as virtual laboratories to design and optimize new materials. This opens up exciting possibilities for large-scale screening studies that can reduce the number of experimental tests, facilitating fast, environmentally friendly and cost-saving computational materials design.

Conclusions

This paper summarizes the progress on hydrogen storage in solids achieved in the framework of the COST Action MP1103. Novel efficient nanomaterials were synthesized, innovative

characterization methods were used to identify the hydrogen sorption reactions and theoretical tools allowed their modeling. More than 50 compounds have been synthesized and characterized; the full range of nanostructure modifications, from nanocavities to nanoparticles, has been exploited to improve the hydrogen sorption properties of the bulk materials. New characterization methods, such as tomography and radiography, were set up and made available to the consortium. More than 100,000 structural combinations were screened via theoretical simulations and complemented the experiments in finding the hydrogen sorption reaction pathways. Numerous collaborations within the European Research communities and beyond were developed because of this important COST Action. The most significant outcomes of these collaborations have been summarized in this publication.

Acknowledgments

REFERENCES

[1] Schlapbach L, Züttel A. Hydrogen-storage materials for mobile applications. Nature 2001;414:353–8.

[2] US. DOE. EERE, Fuel Cell Technologies Program Multi-Year Research, Development and Demonstration Plan, Section 3.3.

[3] Jepsen Lars, Ley Morten B, Young Su-Lee, Cho Young Whan, Dornheim Martin, Jensen Jens Oluf, et al. Boron-nitrogen based hydrides and reactive composites for hydrogen storage. Mater Today 2014;17(3):129–35.

[4] Ley Morten B, Jepsen Lars H, Lee Young-Su, Cho Young Whan, von Colbe José Bellosta, Dornheim Martin, et al. Complex hydrides for hydrogen storage – new perspectives. Mater Today 2014;17(3):122–8.

[5] Cramer CJ, Truhlar DG. Density functional theory for transition metals and transition metal chemistry. Phys Chem Chem Phys 2009;11:10757–816. http://dx.doi.org/10.1039/b907148b.

[6] Cohen AJ, Mori-Sánchez P, Yang W. Challenges for density functional theory. Chem Rev 2012;112:289–320. http://dx.doi.org/10.1021/cr200107z.

[7] Burke K. Perspective on density functional theory. J Chem Phys 2012;136:150901. http://dx.doi.org/10.1063/1.4704546.

[8] Curtarolo S, Hart GLW, Nardelli MB, Mingo N, Sanvito S, Levy O. The high-throughput highway to computational materials design. Nat Mater 2013;12:191–201. http://dx.doi.org/10.1038/nmat3568.

[9] Neugebauer J, Hickel T. Density functional theory in materials science. Wiley Interdiscip Rev Comput Mol Sci 2013;3:438–48. http://dx.doi.org/10.1002/wcms.1125.

[10] Lejaeghere K, Van Speybroeck V, Van Oost G, Cottenier S. Error estimates for solid-state density-functional theory predictions: an overview by means of the ground-state elemental crystals. Crit Rev Solid State Mater Sci 2014;39:1–24. http://dx.doi.org/10.1080/10408436.2013.772503.

[11] Hohenberg P, Kohn W. Inhomogeneous electron gas. Phys Rev 1964;136:B864–71. http://dx.doi.org/10.1103/PhysRev.136.B864.

[12] Kohn W, Sham LJ. Self-consistent equations including exchange and correlation effects. Phys Rev 1965;140:A1133–8. http://dx.doi.org/10.1103/PhysRev.140.A1133.

[13] Shi Q, Voss J, Jacobsen HS, Lefmann K, Zamponi M, Vegge T. Point defect dynamics in sodium aluminum hydrides—A combined quasielastic neutron scattering and density functional theory study. J Alloys Compd 2007;446–447:469–73. http://dx.doi.org/10.1016/j.jallcom.2007.04.041.

[14] Hummelshøj JS, Landis DD, Voss J, Jiang T, Tekin A, Bork N, et al. Density functional theory based screening of ternary alkali-transition metal borohydrides: a computational material design project. J Chem Phys 2009;131:014101. http://dx.doi.org/10.1063/1.3148892.

[15] Huot J, Ravnsbæk DB, Zhang J, Cuevas F, Latroche M, Jensen TR. Mechanochemical synthesis of hydrogen storage materials. Prog Mater Sci 2013;58:30–75.

[16] Zhang J, Cuevas F, Zaïdi W, Bonnet J-P, Aymard L, Bobet J-L, et al. Highlighting of a single reaction path during reactive ball milling of Mg and TM by quantitative H_2 gas sorption analysis to form ternary complex hydrides (TM = Fe, Co, Ni). J Phys Chem C 2011;115:4971–9.

[17] Doppiu S, Schultz L, Gutfleisch O. In situ pressure and temperature monitoring during the conversion of Mg into MgH_2 by high-pressure reactive ball milling. J Alloys Compd 2007;427:204–8.

[18] Deledda S, Hauback BC. The formation mechanism and structural characterisation of the mixed transition-metal complex hydride $Mg_2(FeH_6)_{0.5}(CoH_5)_{0.5}$ obtained by reactive milling. Nanotechnology 2009;20:204010–7.

[19] Polanski M, Nielsen TK, Kunce I, Norek M, Płociński T, Jaroszewicz LR, et al. Mg_2NiH_4 synthesis and decomposition reactions. Int J Hydrogen Energy 2013;38:4003–10.

[20] Norek M, Nielsen TK, Polanski M, Kunce I, Płociński T, Jaroszewicz LR, et al. Synthesis and decomposition mechanisms of ternary Mg_2CoH_5 studied using in situ synchrotron X-ray diffraction. Int J Hydrogen Energy 2011;36(17):10760–70.

[21] Polanski M, Nielsen TK, Cerenius Y, Bystrzycki J, Jensen TR. Synthesis and decomposition mechanisms of Mg_2FeH_6 studied by in-situ synchrotron X-ray diffraction and high-pressure DSC. Int J Hydrogen Energy 2010;35:3578–82.

[22] Mamatha M, Weidenthaler C, Pommerin A, Felderhoff M, Schuth F. Comparative studies of the decomposition of alanates followed by in situ XRD and DSC methods. J Alloys Compd 2006;416:303–14.

[23] Eigen N, Kunowsky M, Klassen T, Bormann R. Synthesis of $NaAlH_4$-based hydrogen storage material using milling under low pressure hydrogen atmosphere. J Alloys Compd 2007;430:350–5.

[24] Jeloaica L, Cuevas-Zhang JX, Cuevas F, Latroche M, Raybaud P. Thermodynamic properties of trialkali (Li, Na, K) hexa-alanates: a combined DFT and experimental study. J Phys Chem C 2008;112:18598–607.

[25] Zhang J, Pilette M-A, Cuevas F, Charpentier T, Mauri F, Latroche M. X-ray diffraction and NMR studies of $Na_{3-n}Li_nAlH_6$ (n = 0, 1, 2) alanates synthesized by high-pressure reactive ball milling. J Phys Chem C 2009;113:21242–52.

[26] Arnbjerg Lene Mosegaard, Jensen Torben R. New compounds in the potassium-aluminium-hydrogen system

observed during release and uptake of hydrogen. Int J Hydrogen Energy 2012;37:345—56.

[27] Li Z, Zhang J, Wang S, Jiang L, Latroche M, Du J, et al. Mechanochemistry of lithium nitride under hydrogen gas. Phys Chem Chem Phys 2015;17:21927—34.

[28] Bellosta von Colbe JM, Felderhoff M, Bogdanovic B, Schuth F, Weidenthaler C. One-step direct synthesis of a Ti-doped sodium alanate hydrogen storage material. Chem Commun 2005:4732—4.

[29] Cuevas F, Korablov D, Latroche M. Synthesis, structural and hydrogenation properties of Mg-rich MgH_2-TiH_2 nanocomposites prepared by reactive ball milling under hydrogen gas. Phys Chem Chem Phys 2012;14:1200—11.

[30] Ponthieu M, Cuevas F, Fernández JF, Laversenne L, Porcher F, Latroche M. Structural properties and reversible deuterium loading of MgD_2-TiD_2 nanocomposites. J Phys Chem C 2013;117:18851—62.

[31] Mirabile Gattia D, Gizer G, Montone A. Effects of the compaction pressure and of the cycling process on kinetics and microstructure of compacted MgH_2-based mixtures. Int J Hydrogen Energy 2014;39:9924—30.

[32] Zhang J, Li Z, Cuevas F, Latroche M. Phase stabilities in the Mg-Si-H system tuned by mechanochemistry". J Phys Chem C 2014;118:21889—95.

[33] Ravnsbæk Dorthe, Filinchuk Yaroslav, Cerenius Yngve, Jakobsen Hans Jørgen, Besenbacher Flemming, Skibsted Jørgen, et al. A series of mixed-metal borohydrides. Angew Chem Int Ed 2009;48:6659—63.

[34] Friedrichs Oliver, Borgschulte Andreas, Kato Shunsuke, Buchter Florian, Gremaud Robin, Remhof Arndt, et al. Low-temperature synthesis of $LiBH_4$ by gas—solid reaction. Chem Eur J 2009;15:5531—4.

[35] Friedrichs O, Remhof A, Borgschulte A, Buchter F, Orimo S, Züttel A. Breaking the passivation—the road to a solvent fee borohydride synthesis. Phys Chem Chem Phys 2010;12:10919—22.

[36] Friedrichs O, Remhof A, Hwang S-J, Züttel A. Role of $Li_2B_{12}H_{12}$ for the Formation and decomposition of $LiBH_4$. Chem Mater 2010;22. 3265—3268 3265.

[37] Frommen C, Sørby MH, Ravindran P, Vajeeston P, Fjellvåg H, Hauback BC. Synthesis, crystal structure, and thermal properties of the first mixed-metal and anion-substituted rare earth borohydride $LiCe(BH_4)_3Cl$. J Phys Chem C 2011:23591—602.

[38] Ley Morten B, Boulineau Sylvain, Janot Raphaël, Filinchuk Yaroslav, Jensen Torben R. New Li ion conductors and solid state hydrogen storage materials: $LiM(BH_4)_3Cl$, M = La or Gd. J Phys Chem C 2012;116:21267—76.

[39] Ley Morten B, Ravnsbæk Dorthe B, Filinchuk Yaroslav, Lee Young-Su, Janot Raphael, Cho Young Whan, et al. $LiCe(BH_4)_3Cl$, a new lithium-ion conductor and hydrogen storage material with isolated tetranuclear anionic clusters. Chem Mater 2012;24:1654—63.

[40] Schouwink Pascal, D'Anna Vincenza, Ley Morten Brix, Daku Latévi Max Lawson, Richter Bo, Jensen Torben R, et al. Bimetallic borohydrides in the system $M(BH_4)_2$ — KBH_4 (M = Mg, Mn): on the structural diversity. J Phys Chem C 2012;116:10829—40.

[41] Černý Radovan, Schouwink Pascal, Sadikin Yolanda, Stare Katarina, Smrčok Ľubomír, Richter Bo, et al. Trimetallic borohydride $Li_3MZn_5(BH_4)_{15}$ (M = Mg, Mn), containing two weakly interconnected frameworks. Inorg Chem 2013;52:9941—7.

[42] Skripov Alexander V, Soloninin Alexei V, Ley Morten B, Jensen Torben R, Filinchuk Yaroslav. Nuclear magnetic resonance studies of BH_4 reorientations and Li diffusion in $LiLa(BH_4)_3Cl$. J Phys Chem C 2013;117:14965—72.

[43] Schouwink Pascal, Ley Morten B, Tissot Antoine, Hagemann Hans, Jensen Torben R, Smrčok Lubomir, et al. Structure and properties of complex hydride perovskite material. Nat Comm 2014;5:5706.

[44] Schouwink P, Ley MB, Jensen TR, Smrčok L, Černý R. Borohydrides: from sheet to framework topologies. Dalton Trans 2014;43:7726—33.

[45] Sadikin Yolanda, Stare Katarina, Schouwink Pascal, Ley Morten Brix, Jensen Torben R, Meden Anton, et al. Alkali metal — yttrium borohydrides: the link between coordination of small and large rare-earth. J Solid State Chem 2015;225:231—9.

[46] Paskevicius Mark, Ley Morten B, Sheppard Drew A, Jensen Torben R, Buckley Craig E. Eutectic melting in metal borohydrides. Phys Chem Chem Phys 2013;15:19774—89.

[47] Ley Morten B, Paskevicius Mark, Schouwink Pascal, Richter Bo, Sheppard Drew A, Buckley Craig E, et al. Novel solvates $M(BH_4)_3S(CH_3)_2$ and properties of halide-free $M(BH_4)_3$ (M = Y or Gd). Dalton Trans 2014;43(35):13333—42.

[48] Ley Morten B, Roedern Elsa, Thygesen Peter MM, Jensen Torben R. Melting behaviour and thermolysis of NaBH4—$Mg(BH_4)_2$ and NaBH4—$Ca(BH_4)_2$ composites. Energies 2015;8:2701—13. http://dx.doi.org/10.3390/en8042701.

[49] Moury R, Demirci U, Ban V, Filinchuk Y, Ichikawa T, Zeng L, et al. Lithium hydrazinidoborane: a polymorphic material with potential for chemical hydrogen storage. Chem Mater 2014;26(10):3249—55.

[50] Moury R, Demirci UB, Ichikawa T, Filinchuk Y, Chiriac R, van der Lee A, et al. Sodium hydrazinidoborane: a chemical hydrogen-storage material. ChemSusChem 2013;6(4):667—73.

[51] Dovgaliuk I, Ban V, Sadikin Y, Cerný R, Aranda L, Casati N, et al. The first halide-free bimetallic aluminum borohydride: synthesis, structure, stability, and decomposition pathway. J Phys Chem C 2014;118(1):145—53.

[52] Schouwink P, Morelle F, Sadikin Y, Filinchuk Y, Cerný R. Increasing hydrogen density with the cation-anion pair BH_4^--NH_4^+ in perovskite-type $NH_4Ca(BH_4)_3$. Energies 2015;8(8):8286—99.

[53] Humphries Terry D, Ley Morten B, Frommen Christoph, Munroe Keelie T, Jensen Torben R, Hauback Bjørn C. Crystal Structure and in situ decomposition of $Eu(BH_4)_2$ and $Sm(BH_4)_2$. J Mater Chem A 2015;3:691—8.

[54] Richter Bo, Ravnsbæk Dorthe B, Tumanov Nikolay, Filinchuk Yaroslav, Jensen Torben R. Manganese borohydride; synthesis and characterization. Dalton Trans 2015;44:3988—96.

[55] Tumanov Nikolay A, Safin Damir A, Richter Bo, Jensen Torben R, Garcia Yann, Filinchuk Yaroslav. Challenges in the synthetic routes to $Mn(BH_4)_2$: insight into intermediate compounds. Dalton 2015;44:6571—80.

[56] Jepsen Lars H, Ley Morten B, Filinchuk Yaroslav, Besenbacher Flemming, Jensen Torben R. Tailoring the properties of ammine metal borohydrides for solid-state hydrogen storage. ChemSusChem 2015;8:1452—63.

[57] Jepsen Lars H, Lee Young-Su, Černý Radovan, Sarusie Ram S, Cho Young Whan, Besenbacher Flemming, et al. Ammine calcium and strontium borohydrides: syntheses, structures and properties. ChemSusChem 2015;8:3472—82.

[58] Jepsen LH, Ban V, Møller K, Lee Y-S, Cho YW, Besenbacher F, et al. Synthesis, crystal structure, thermal decomposition and ^{11}B MAS NMR characterization of $Mg(BH_4)_2(NH_3BH_3)_2$. J Phys Chem C 2014;118:12141—53.

[59] Dovgaliuk I, Le Duff CS, Robeyns K, Devillers M, Filinchuk Y. Mild dehydrogenation of ammonia borane complexed with aluminum borohydride. Chem Mater 2015;27:768—77.

[60] Ban V, Soloninin AV, Skripov AV, Hadermann J, Abakumov A, Filinchuk Y. Pressure-collapsed amorphous $Mg(BH_4)_2$: an ultradense complex hydride showing a reversible transition to the porous framework. J Phys Chem C 2014;118:23402–8.

[61] Tumanov NA, Roedern E, Lodziana Z, Nielsen DB, Jensen TR, Talyzin AV, et al. High-pressure study of $Mn(BH_4)_2$ reveals a stable polymorph with high hydrogen density. Chem Mater 2016;28:274–83.

[62] Calizzi M, Venturi F, Ponthieu M, Cuevas F, Morandi V, Perkisas T, et al. Gas-phase synthesis of Mg-Ti nanoparticles for solid-state hydrogen storage. Phys Chem Chem Phys 2016;18:141–8.

[63] Mooij LPA, Baldi A, Boelsma C, Shen K, Wagemaker M, Pivak Y, et al. Interface energy controlled thermodynamics of nanoscale metal hydrides. Adv Energy Mater 2011;1:754–8.

[64] Mooij Lennard, Perkisas Tyche, Palsson Gunnar, Schreuders Herman, Wolff Max, Hjorvarsson Bjorgvin, et al. The effect of microstructure on the hydrogenation of Mg/Fe thin film multilayers. Int J Hydrogen Energy 2014;39:17092–103.

[65] Mooij L, Dam B. Hysteresis and the role of nucleation and growth in the hydrogenation of Mg nanolayers. Phys Chem Chem Phys 2013;15:2782.

[66] Mooij L, Dam B. Nucleation and growth mechanisms of nano-magnesium hydride from the Hydrogen sorption kinetics. Phys Chem Chem Phys 2013;15:11501–10.

[67] Schlichtenmayer M, Hirscher M. Nanosponges for hydrogen storage. J Mater Chem 2012;22:10134–43.

[68] Klein N, Senkovska I, Baburin IA, Grünker R, Stoeck U, Schlichtenmayer M, et al. Route to a family of robust, non-interpenetrated metal-organic frameworks with pto-like topology. Chem A Eur J 2011;17:13007–16.

[69] Streppel B, Hirscher M. BET specific surface area and pore structure of MOFs determined by hydrogen adsorption at 20 K. Phys Chem Chem Phys 2011;13:3220–2.

[70] Oh H, Lupu D, Blanita G, Hirscher M. Experimental assessment of Physical upper limit for hydrogen storage capacity at 20 K in densified MIL-101 monoliths. RSC Adv 2014;4:2648–51.

[71] Dinca M, Long JR. High-enthalpy hydrogen adsorption in cation-exchanged variants of the microporous metal−organic framework $Mn_3[(Mn_4Cl)_3(BTT)_8(CH_3OH)_{10}]_2$. J Am Chem Soc 2007;129:11172–6.

[72] Szilágyi PÁ, Weinrauch I, Oh H, Hirscher M, Juan-Alcañiz J, Serra-Crespo P, et al. Interplay of linker functionalization and hydrogen adsorption in the metal−organic framework MIL-101. J Phys Chem C 2014;118:19572–9.

[73] Filinchuk Y, Richter B, Jensen TR, Dmitriev V, Chernyshov D, Hagemann H. Porous and dense magnesium borohydride frameworks: synthesis, stability, and reversible absorption of guest species. Angew Chem Int Ed 2011;50:11162–6.

[74] Roduner E. Size matters: why nanomaterials are different. Chem Soc Rev 2006;35:583–92.

[75] Hu W, Xiao S, Deng H, Luo W, Deng L. Thermodynamic properties of nano-silver and alloy particles. In: PozoPerez D, editor. Silver nanoparticles. Vukovar, Croatia: InTech; 2010. p. 1–3.

[76] Hashmi ASK, Hutchings GJ. Gold catalysis. Angew Chem Int Ed 2006;45:7896–936.

[77] Lai Q, Paskevicius M, Sheppard DA, Buckley CE, Thornton AW, Hill MR, et al. Hydrogen storage materials for mobile and stationary applications: current state of the art. ChemSusChem 2015;8:2789–825.

[78] Zlotea C, Latroche M. Role of nanoconfinement on hydrogen sorption properties of metal nanoparticles hybrids. Colloid Surfaces A Physicochem Eng Aspects 2013;439:117–30.

[79] de Jongh PE, Adelhelm P. Nanosizing and nanoconfinement: new strategies towards meeting hydrogen storage goals. Chemsuschem 2010;3:1332–48.

[80] Nielsen TK, Besenbacher F, Jensen TR. Nanoconfined hydrides for energy storage. Nanoscale 2011;3:2086–98.

[81] Pasquini L, Callini E, Piscopiello E, Montone A, VittoriAntisari M, Bonetti E. Metal-hydride transformation kinetics in magnesium nanoparticles. Appl Phys Lett 2009;94:041918.

[82] Vons VA, Anastasopol A, Legerstee WJ, Mulder FM, Eijt SWH, Schmidt-Ott A. Low-temperature hydrogen desorption and the structural properties of spark discharge generated Mg nanoparticles. Acta Mater 2011;59:3070–80.

[83] Krishnan G, Negrea RF, Ghica C, ten Brink GH, Kooi BJ, Palasantzas G. Synthesis and exceptional thermal stability of Mg-based bimetallic nanoparticles during hydrogenation. Nanoscale 2014;6:11963.

[84] Pasquini L, Sacchi M, Brighi M, Boelsma C, Bals S, Perkisas T, et al. Hydride destabilization in core-shell nanoparticles. Int J Hydrogen Energy 2014;39:2115–23.

[85] Venturi F, Calizzi M, Bals S, Perkisas T, Pasquini L. Self-assembly of gas-phase synthesized magnesium nanoparticles on room temperature substrates. Mater Res Express 2015;2:015007.

[86] Au YS, Obbink MK, Srinivasan S, Magusin PCMM, de Jong KP, de Jongh PE. The size dependence of hydrogen mobility and sorption kinetics for carbon-supported MgH_2 particles. Adv Funct Mater 2014;24:3604–11.

[87] Aguey-Zinsou KF, Fernandez JRA, Klassen T, Bormann R. Effect of Nb_2O_5 on MgH_2 properties during mechanical milling. Int J Hydrogen Energy 2007;32:2400–7.

[88] Zlotea C, Chevalier-César C, Léonel E, Leroy E, Cuevas F, Dibandjo P, et al. Synthesis of small metallic Mg-based nanoparticles confined in porous carbon materials for hydrogen sorption. Faraday Disc 2011;151:117–31.

[89] Baldé CP, Hereijgers BPC, Bitter JH, de Jong KP. Facilitated hydrogen storage in $NaAlH_4$ supported on carbon nanofibers. Angew Chem Int Ed 2006;45:3501–3.

[90] Nielsen TK, Javadian P, Polanski M, Besenbacher F, Bystrzycki J, Skibsted J, et al. Nanoconfined $NaAlH_4$: prolific effects from increased surface area and pore volume. Nanoscale 2014;6:599–607.

[91] Ngene P, van den Berg R, Verkuijlen MHW, de Jong KP, de Jongh PE. Reversibility of the hydrogen desorption from $NaBH_4$ by confinement in nanoporous carbon. Energy Environ Sci 2011;4:4108–15.

[92] Gross AF, Vajo JJ, Van Atta SL, Olson GL. Enhanced hydrogen storage kinetics of $LiBH_4$ in nanoporous carbon scaffolds. J Phys Chem C 2008;112:5651–7.

[93] Christian ML, Aguey-Zinsou K-FO. Core−shell strategy leading to high reversible hydrogen storage capacity for $NaBH_4$. ACS Nano 2012;6:7739–51.

[94] Ngene P, Verkuijlen MHW, Zheng Q, Kragten J, van Bentum PJM, Bitter JH, et al. The role of Ni in increasing the reversibility of the hydrogen release from nanoconfined LiBH4. Faraday Discuss 2011;151:47–58.

[95] Li Y, Zhou G, Fang F, Yu X, Zhang Q, Ouyang L, et al. De-re-hydrogenation features of $NaAlH_4$ confined exclusively in nanopores. Acta Mater 2011;59:1829–38.

[96] Gao J, Ngene P, Herrich M, Xia W, Gutfleisch O, Muhler M, et al. Interface effects in $NaAlH_4$−carbon nanocomposites for hydrogen storage. Int J Hydrogen Energy 2014;39:10175–83.

[97] Moussa G, Demirci UB, Malo S, Bernard S, Miele P. Hollow core@mesoporous shell boron nitride nanopolyhedron-confined ammonia borane: a pure B-N-H composite for chemical hydrogen storage. J Mater Chem A 2014;2:7717–22.

[98] Gao J, Adelhelm P, Verkuijlen MHW, Rongeat C, Herrich M, van Bentum PJM, et al. Confinement of NaAlH₄ in nanoporous carbon: impact on H2 release, reversibility, and thermodynamics. J Phys Chem C 2010;114:4675–82.

[99] Chua YS, Chen P, Wu G, Xiong Z. Development of amidoboranes for hydrogen storage. Chem Commun 2011;47:5116–29.

[100] Chua YS, Li W, Wu G, Xiong Z, Chen P. From exothermic to endothermic dehydrogenation – interaction of monoammoniate of magnesium amidoborane and metal hydrides. Chem Mater 2012;24:3574–81.

[101] Chua YS, Wu H, Zhou W, Udovic TJ, Wu G, Xiong Z, et al. Monoammoniate of calcium amidoborane: synthesis, structure, and hydrogen-storage properties. Inorg Chem 2012;51:1599–603.

[102] Wu C, Wu G, Xiong Z, Han X, Chu H, He T, et al. LiNH₂BH₃·NH₃BH₃: structure and hydrogen storage properties. Chem Mater 2010;22:3–5.

[103] Wu H, Zhou W, Pinkerton FE, Meyer MS, Yao Q, Gadipelli S, et al. Sodium magnesium amidoborane: the first mixed-metal amidoborane. Chem Commun 2011;47:4102–4204Pubmed.

[104] Biliškov N, Halasz I, Callini E, Borgschulte A, Züttel A. Synthesis and characterisation of new amidoboranes. In: Proc. 9th Int. Symp. Hydrogen & Energy, Emmetten, Switzerland; 2015. p. 28.

[105] Fijalkowski KJ, Genova RV, Filinchuk Y, Budzianowski A, Derzci M, Jaroń T, et al. Na[Li(NH₂BH₃)₂] – the first mixed-cation amidoborane with unusual crystal structure. Dalton Trans 2011;40:4407–13.

[106] Dovgaliuk I, Jepsen LH, Safin DA, Lodziana Z, Dyadkin V, Jensen TR, et al. A composite of complex and chemical hydrides yields the first Al-Based amidoborane with improved hydrogen storage properties. Chem Eur J 2015:14562–70.

[107] Meilikhov M, Yusenko K, Esken D, Turner S, Van Tendeloo G, Fischer RA. Metals@ MOFs–loading MOFs with metal nanoparticles for hybrid functions. Eur J Inorg Chem 2010;2010:3701–14.

[108] Turner S, Lebedev OI, Schröder F, Esken D, Fischer RA, Tendeloo GV. Direct imaging of loaded metal– organic framework materials (metal@ MOF-5). Chem Mater 2008;20:5622–7.

[109] Wiktor C, Turner S, Zacher D, Fischer RA, Van Tendeloo G. Imaging of intact MOF-5 nanocrystals by advanced TEM at liquid nitrogen temperature. Microporous Mesoporous Mater 2012;162:131–5.

[110] Kalidindi SB, Oh H, Hirscher M, Esken D, Wiktor C, Turner S, et al. Metal@ COFs: covalent organic frameworks as templates for Pd nanoparticles and hydrogen storage properties of Pd@ COF-102 hybrid material. Chem A Eur J 2012;18:10848–56.

[111] Hadermann J, Abakumov A, Van Rompaey S, Perkisas T, Filinchuk Y, Van Tendeloo G. Crystal structure of a lightweight borohydride from submicrometer crystallites by precession electron diffraction. Chem Mater 2012;24(17):3401–5.

[112] Broom DP. Hydrogen storage materials: the characterisation of their storage properties. Springer Science & Business Media; 2011.

[113] Broom DP, Webb CJ, Hurst KE, Parilla PA, Gennett T, Brown CM, et al. Outlook and challenges for hydrogen storage in nanoporous materials. Appl Phys A 2016;122:151.

[114] Zhou W, Wu H, Hartman MR, Yildirim T. Hydrogen and methane adsorption in metal-organic frameworks: a high-pressure volumetric study. J Phys Chem C 2007;111:16131–7.

[115] Myers A, Monson P. Adsorption in porous materials at high pressure: theory and experiment. Langmuir 2002;18:10261–73.

[116] Ozdemir E, Morsi BI, Schroeder K. Importance of volume effects to adsorption isotherms of carbon dioxide on coals. Langmuir 2003;19:9764–73.

[117] Spanopoulos I, Bratsos I, Tampaxis Ch, Kourtellaris A, Charalambopoulou G, Steriotis TA, et al. Enhanced gas-sorption properties of a high surface area, ultramicroporous magnesium formate. CrystEngComm 2015;17:532–9.

[118] Møller KT, Hansen BR, Dippel AC, Jørgensen JE, Jensen TR. Characterization of gas-solid reactions using in situ powder X-ray diffraction. Z Anorg Allg Chem 2014;640:3029–43.

[119] Hansen BR, Møller KT, Paskevicius M, Dippel A-C, Walter P, Webb CJ, et al. In situ X-ray diffraction environments for high-pressure reactions. J Appl Crystallogr 2015;48:1234–41.

[120] Jensen TR, Nielsen TK, Filinchuk Y, Jørgensen J-E, Cerenius Y, Gray EM, et al. Versatile in situ powder X-ray diffraction cells for solid–gas investigations. J Appl Crystallogr 2010;43:1456–63.

[121] Pistidda C, Santoru A, Garroni S, Bergemann N, Rzeszutek A, Horstmann C, et al. First direct study of the ammonolysis reaction in the most common alkaline and alkaline earth metal hydrides by in situ SR-PXD. J Phys Chem C 2015;119:934–43.

[122] Ravnsbæk DB, Filinchuk Y, Cerný R, Jensen TR. Powder diffraction methods for studies of borohydride-based energy storage materials. Z Kristallogr Cryst Mater 2010;225:557–69.

[123] Rude LH, Nielsen TK, Ravnsbaek DB, Bösenberg U, Ley MB, Richter B, et al. Tailoring properties of borohydrides for hydrogen storage: a review. Phys status Solidi (a) 2011;208:1754–73.

[124] Ley MB, Roedern E, Jensen TR. Eutectic melting of LiBH₄–KBH₄. Phys Chem Chem Phys 2014;16:24194–9.

[125] Nickels EA, Jones MO, David WI, Johnson SR, Lowton RL, Sommariva M, et al. Tuning the decomposition temperature in complex hydrides: synthesis of a mixed alkali metal borohydride. Angew Chem Int Ed 2008;47:2817–9.

[126] Filinchuk Y, Tumanov NA, Ban V, Ji H, Wei J, Swift MW, et al. Situ diffraction study of catalytic hydrogenation of VO₂: stable phases and origins of metallicity. J Am Chem Soc 2014;136(22):8100–9.

[127] Trenary M. Surface and thin film analysis. A compendium of principles, instrumentation, and applications. Weinheim, Germany: Wiley-VCH; 2003.

[128] Barawi M, Granero C, Diaz-Chao P, Manzano C, Martin-Gonzalez M, Jimenez-Rey D, et al. Thermal decomposition of non-catalysed MgH₂ films. Int J Hydrogen Energy 2014;39:9865–70.

[129] Ares J, Leardini F, Díaz-Chao P, Ferrer I, Fernández J, Sánchez C. Non-isothermal desorption process of hydrogenated nanocrystalline Pd-capped Mg films investigated by Ion Beam Techniques. Int J Hydrogen Energy 2014;39:2587–96.

[130] Kótai E. Computer methods for analysis and simulation of RBS and ERDA spectra. Nucl Instrum Methods Phys Res Sect B Beam Interact Mater Atoms 1994;85:588–96.

[131] Barkhordarian G, Klassen T, Dornheim M, Bormann R. Unexpected kinetic effect of MgB₂ in reactive hydride composites containing complex borohydrides. J Alloys Compd 2007;440:L18–21.

[132] Vajo JJ, Skeith SL, Mertens F. Reversible storage of hydrogen in destabilized LiBH₄. J Phys Chem B 2005;109:3719–22.

[133] Kissinger HE. Reaction kinetics in differential thermal analysis. Anal Chem 1957;29:1702–6.

[134] Chaudhary A-L, Sheppard DA, Paskevicius M, Pistidda C, Dornheim M, Buckley CE. Reaction kinetic behaviour with relation to crystallite/grain size dependency in the Mg–Si–H system. Acta Mater 2015;95:244–53.

[135] Chaudhary A-L, Li G, Matsuo M, Orimo S-i, Deledda S, Sørby MH, et al. Simultaneous desorption behavior of M borohydrides and Mg_2FeH_6 reactive hydride composites (M = Mg, then Li, Na, K, Ca). Appl Phys Lett 2015;107:073905.

[136] Chaudhary A-L, Paskevicius M, Sheppard DA, Buckley CE. Thermodynamic destabilisation of MgH_2 and $NaMgH_3$ using group IV elements Si, Ge or Sn. J Alloys Compd 2015;623:109–16.

[137] Jepsen J, Milanese C, Girella A, Lozano GA, Pistidda C, Bellosta Von Colbe JM, et al. Compaction pressure influence on material properties and sorption behaviour of $LiBH_4$-MgH_2 composite. Int J Hydrogen Energy 2013;38:8357–66.

[138] Pohlmann C, Röntzsch L, Hu J, Weißgärber T, Kieback B, Fichtner M. Tailored heat transfer characteristics of pelletized $LiNH_2$–MgH_2 and $NaAlH_4$ hydrogen storage materials. J Power Sources 2012;205:173–9.

[139] Pranzas PK, Bösenberg U, Karimi F, Münning M, Metz O, Minella CB, et al. Characterization of hydrogen storage materials and systems with photons and neutrons. Adv Eng Mater 2011;13:730–6.

[140] Pohlmann C, Röntzsch L, Kalinichenka S, Hutsch T, Kieback B. Magnesium alloy-graphite composites with tailored heat conduction properties for hydrogen storage applications. Int J Hydrogen Energy 2010;35:12829–36.

[141] Pohlmann C, Röntzsch L, Kalinichenka S, Hutsch T, Weißgärber T, Kieback B. Hydrogen storage properties of compacts of melt-spun $Mg_{90}Ni_{10}$ flakes and expanded natural graphite. J Alloys Compd 2011;509:S625–8.

[142] Chaise A, De Rango P, Marty P, Fruchart D, Miraglia S, Olives R, et al. Enhancement of hydrogen sorption in magnesium hydride using expanded natural graphite. Int J Hydrogen Energy 2009;34:8589–96.

[143] Nachev S, De Rango P, Delhomme B, Planté D, Zawilski B, Longa F, et al. In situ dilatometry measurements of MgH_2 compacted disks. J Alloys Compd 2013;580:S183–6.

[144] Shim J-H, Park M, Lee YH, Kim S, Im YH, Suh J-Y, et al. Effective thermal conductivity of MgH_2 compacts containing expanded natural graphite under a hydrogen atmosphere. Int J Hydrogen Energy 2014;39:349–55.

[145] Mirabile Gattia D, Montone A, Pasquini L. Microstructure and morphology changes in MgH_2/expanded natural graphite pellets upon hydrogen cycling. Int J Hydrogen Energy 2013;38:1918–24.

[146] Lozano GA, Ranong CN, Bellosta Von Colbe JM, Bormann R, Hapke J, Fieg G, et al. Optimization of hydrogen storage tubular tanks based on light weight hydrides. Int J Hydrogen Energy 2012;37:2825–34.

[147] Börries S, Metz O, Pranzas P, Bücherl T, Söllradl S, Dornheim M, et al. Scattering influences in quantitative fission neutron radiography for the in situ analysis of hydrogen distribution in metal hydrides. Nucl Instrum Methods Phys Res Sect A Accel Spectrom Detect Assoc Equip 2015;797:158–64.

[148] Jensen PB, Lysgaard S, Quaade UJ, Vegge T. Designing mixed metal halide ammines for ammonia storage using density functional theory and genetic algorithms. Phys Chem Chem Phys 2014;16:19732–40. http://dx.doi.org/10.1039/c4cp03133d.

[149] Jensen PB, Bialy A, Blanchard D, Lysgaard S, Reumert AK, Quaade UJ, et al. Accelerated DFT-based design of materials for ammonia storage. Chem Mater 2015. http://dx.doi.org/10.1021/acs.chemmater.5b00446. 150603150920000.

[150] Paskaš Mamula B, Grbović Novaković J, Radisavljević I, Ivanović N, Novaković N. Electronic structure and charge

[150] distribution topology of MgH_2 doped with 3d transition metals. Int J Hydrogen Energy 2014;39:5874–87. http://dx.doi.org/10.1016/j.ijhydene.2014.01.172.

[151] Holland JH. Adaptation in natural and artificial systems. Ann Arbor: University of Michigan Press; 1975.

[152] Forrest S. Genetic algorithms: principles of natural selection applied to computation. Sci (80-) 1993;261:872–8. http://dx.doi.org/10.1126/science.8346439.

[153] Deaven DM, Ho KM. Molecular-geometry optimization with a genetic algorithm. Phys Rev Lett 1995;75:288–91.

[154] Lysgaard S, Landis DD, Bligaard T, Vegge T. Genetic algorithm procreation operators for alloy nanoparticle catalysts. Top Catal 2014;57:33–9. http://dx.doi.org/10.1007/s11244-013-0160-9.

[155] Lysgaard S, Mýrdal JSG, Hansen HA, Vegge T. DFT-based genetic algorithm search for AuCu nanoalloy electrocatalysts for CO_2 reduction. Phys Chem Chem Phys 2015;27:4552–61.

[156] Klerke A, Christensen CH, Nørskov JK, Vegge T. Ammonia for hydrogen storage: challenges and opportunities. J Mater Chem 2008;18:2304–10. http://dx.doi.org/10.1039/b720020j.

[157] Sørensen RZ, Hummelshøj JS, Klerke A, Reves JB, Vegge T, Nørskov JK, et al. Indirect, reversible high-density hydrogen storage in compact metal ammine salts. J Am Chem Soc 2008;130:8660–8. http://dx.doi.org/10.1021/ja076762c.

[158] Hussain T, Pathak B, Ramzan M, Maark TA, Ahuja R. Calcium doped graphane as a hydrogen storage material. Appl Phys Lett 2012;100(183902):1–5.

[159] Hussain T, Pathak B, Maark TA, Araujo Araujo CM, Scheicher RH, Ahuja R. Ab initio study of lithium-doped graphane for hydrogen storage. Eur Phys Lett 2011;96(27013):p1–4.

[160] Hussain T, Chakraborty S, Ahuja R. Metal-functionalized silicene for efficient hydrogen storage. ChemPhysChem 2013;14:3463–6.

[161] Hussain T, Kaewmaraya T, Chakraborty S, Ahuja R. Functionalization of hydrogenated silicene with alkali and alkaline earth metals for efficient hydrogen storage. Phys Chem Chem Phys 2013;15:18900.

[162] Orimo S-I, Nakamori Y, Eliseo JR, Züttel A, Jensen CM. Complex hydrides for hydrogen storage. Chem Rev 2007;107:4111–32. http://dx.doi.org/10.1021/cr0501846.

[163] Sakintuna B, Lamari-Darkrim F, Hirscher M. Metal hydride materials for solid hydrogen storage: a review. Int J Hydrogen Energy 2007;32:1121–40. http://dx.doi.org/10.1016/j.ijhydene.2006.11.022.

[164] Churchard AJ, Banach E, Borgschulte A, Caputo R, Chen J-C, Clary D, et al. A multifaceted approach to hydrogen storage. Phys Chem Chem Phys 2011:16955–72. http://dx.doi.org/10.1039/c1cp22312g.

[165] Biliškov N, Miletić GI, Drašner A. Structural and hydrogen sorption properties of $SmNi_{5-x}Ga_x$ system − an experimental and theoretical study. Int J Hydrogen Energy 2013;38:12213–22. http://dx.doi.org/10.1016/j.ijhydene.2013.05.154.

[166] Biliškov N, Miletić GI, Drašner A, Prezelj K. Structural and hydrogen sorption properties of $SmNi_{5-x}Al_x$ system − an experimental and theoretical study. Int J Hydrogen Energy 2015;40:8548–61. http://dx.doi.org/10.1016/j.ijhydene.2015.04.076.

[167] Christensen CH, Sørensen RZ, Johannessen T, Quaade UJ, Honkala K, Elmøe TD, et al. Metal ammine complexes for hydrogen storage. J Mater Chem 2005;15:4106–8. http://dx.doi.org/10.1039/b511589b.

[168] Vegge T, Sørensen RZ, Klerke A, Hummelshøj JS, Johannessen T, Nørskov JK, et al. Indirect hydrogen storage in metal ammines. In: Walker G, editor. Solid state Hydrog.

storage Mater. Chem. British Welding Research Association; 2008. p. 533–68.

[169] Tekin A, Hummelshøj JS, Jacobsen HS, Sveinbjörnsson D, Blanchard D, Nørskov JK, et al. Ammonia dynamics in magnesium ammine from DFT and neutron scattering. Energy Environ Sci 2010;3:448–56. http://dx.doi.org/10.1039/b921442a.

[170] Ammitzboll AL, Lysgaard S, Klukowska A, Vegge T, Quaade UJ. Surface adsorption in strontium chloride ammines. J Chem Phys 2013;138:164701. http://dx.doi.org/10.1063/1.4800754.

[171] Lysgaard S, Ammitzbøll AL, Johnsen RE, Norby P, Quaade UJ, Vegge T. Resolving the stability and structure of strontium chloride amines from equilibrium pressures, XRD and DFT. Int J Hydrogen Energy 2012;37:18927–36. http://dx.doi.org/10.1016/j.ijhydene.2012.09.129.

[172] Johnsen RE, Jensen PB, Norby P, Vegge T. Temperature and pressure induced changes in the crystal structure of $Sr(NH_3)_8Cl_2$. J Phys Chem C 2014;118:24349–56. http://dx.doi.org/10.1021/jp508076c.

[173] Dion M, Rydberg H, Schröder E, Langreth DC, Lundqvist BI. Van der Waals Density Functional for General Geometries. Phys Rev Lett 2004;92:246401. http://dx.doi.org/10.1103/PhysRevLett.92.246401.

[174] Bialy A, Jensen PB, Blanchard D, Vegge T, Quaade UJ. Solid solution barium–strontium chlorides with tunable ammonia desorption properties and superior storage capacity. J Solid State Chem 2015;221:32–6. http://dx.doi.org/10.1016/j.jssc.2014.09.014.

[175] Vegge T. Locating the rate-limiting step for the interaction of hydrogen with Mg (0001) using density-functional theory calculations and rate theory. Phys Rev B 2004;70:035412. http://dx.doi.org/10.1103/PhysRevB.70.035412.

[176] Kurko S, Paskaš-mamula B, Matović L, Novaković JG, Novaković N. The influence of boron doping concentration on MgH_2 electronic structure. Acta Phys Pol A 2011;120:238–41.

[177] Hussain T, Sarkar A De, Maark TA, Sun W, Ahuja R. Strain and doping effects on the energetics of hydrogen desorption from the MgH_2 (001) surface. EPL (Europhysics Lett) 2013;101:27006. http://dx.doi.org/10.1209/0295-5075/101/27006.

[178] Hussain T, Maark TA, Pathak B, Ahuja R, Maark A. Improvement in the hydrogen desorption from MgH_2 upon transition metals doping: a hybrid density functional calculations. AIP Adv 2013;102117:0–8. http://dx.doi.org/10.1063/1.4826521.

[179] Sun W, Hussain T, De Sarkar A, Maark TA, Luo W, Ahuja R. Improvement in the desorption of H_2 from the MgH_2 (1 1 0) surface by means of doping and mechanical strain. Comput Mater Sci 2014;86:165–9. http://dx.doi.org/10.1016/j.commatsci.2014.01.029.

[180] Giusepponi S, Celino M. DFT model of hydrogen desorption from MgH_2: the role of iron catalyst. Int J Hydrogen Energy 2013;38:15254–63. http://dx.doi.org/10.1016/j.ijhydene.2013.09.132.

[181] Larsson P, Araújo CM, Larsson JA, Jena P, Ahuja R. Role of catalysts in dehydrogenation of MgH_2 nanoclusters. Proc Natl Acad Sci U S A 2008;105:8227–31. http://dx.doi.org/10.1073/pnas.0711743105.

[182] Kurko Sandra, Milanovic Igor, Grbovic Novakovic Jasmina, Ivanovic Nenad, Novakovic Nikola. Investigation of surface and near-surface effects on hydrogen desorption kinetics of MgH_2. Int J Hydrogen Energy 2014;39(2):862–7.

[183] Hussain T, Sarkar AD, Ahuja R. Strain induced lithium functionalized graphane as a high capacity hydrogen storage material. Appl Phys Lett 2012;101(103907):1–5.

[184] Hussain T, Chakraborty S, Sarkar AD, Johansson B, Ahuja R. Enhancement of energy storage capacity of Mg functionalized silicene and silicane under external strain. Appl Phys Lett 2014;105:123903.

[185] Zarkevich NA, Majzoub EH, Johnson DD. Anisotropic thermal expansion in molecular solids: theory and experiment on $LiBH_4$. Phys Rev B 2014;89:134308. http://dx.doi.org/10.1103/PhysRevB.89.134308.

[186] Saldan I. A prospect for LiBH4 as on-board hydrogen storage. Cent Eur J Chem 2011;9:761–75. http://dx.doi.org/10.2478/s11532-011-0068-9.

[187] Blanchard D, Nale A, Sveinbjörnsson D, Eggenhuisen TM, Verkuijlen MHW, Vegge T, et al. Nanoconfined $LiBH_4$ as a fast lithium ion conductor. Adv Funct Mater 2015;25:184–92. http://dx.doi.org/10.1002/adfm.201402538.

[188] Łodziana Z, Błoński P, Yan Y, Rentsch D, Remhof A. NMR chemical shifts of 11B in metal borohydrides from first-principle calculations. J Phys Chem C 2014;118:6594–603. http://dx.doi.org/10.1021/jp4120833.

[189] Łodziana Z, Błoński P. Structure of nanoconfined LiBH4 from first principles ^{11}B NMR chemical shifts calculations. Int J Hydrogen Energy 2014;39:9842–7. http://dx.doi.org/10.1016/j.ijhydene.2014.02.150.

[190] Błoński P, Łodziana Z. First-principles study of $LiBH_4$ nanoclusters interaction with models of porous carbon and silica scaffolds. Int J Hydrogen Energy 2014;39:9848–53. http://dx.doi.org/10.1016/j.ijhydene.2014.03.264.

[191] Li Y, Hussain T, Sarkar AD, Ahuja R. Hydrogen storage in polylithiated BC3 monolayer sheet. Solid State Commun 2013;170:39.

[192] Hussain T, Chakraborty S, Kang TW, Johansson B, Ahuja R. BC_3 sheet functionalized with lithium rich species emerging as a reversible hydrogen storage material. ChemPhysChem 2015;16:634.

[193] Hussain T, Maark TA, Sarkar AD, Ahuja R. Polylithiated (OLi_2) functionalized graphane as a potential hydrogen storage material. Appl Phys Lett 2012;101:243902.

[194] Hussain T, Sarkar AD, Johansson B, Ahuja R. Functionalization of hydrogenated graphene by polylithiated species for efficient hydrogen storage. Int J Hydrogen Energy 2014;39:2560–6.